NACA

RESEARCH MEMORANDUM

BOUNDARY-LAYER-TRANSITION AND HEAT-TRANSFER MEASUREMENTS

FROM FLIGHT TESTS OF BLUNT AND SHARP 50° CONES

AT MACH NUMBERS FROM 1.7 TO 4.7

By Leo T. Chauvin and Katherine C. Speegle

Langley Aeronautical Laboratory
Langley Field, Va.

NATIONAL ADVISORY COMMITTEE
FOR AERONAUTICS

WASHINGTON

[redacted]

BOUNDARY-LAYER-TRANSITION AND HEAT-TRANSFER MEASUREMENTS FROM FLIGHT TESTS OF BLUNT AND SHARP 50° CONES AT MACH NUMBERS FROM 1.7 TO 4.7

By Leo T. Chauvin and Katherine C. Speegle

ABSTRACT

Boundary-layer-transition and heat-transfer measurements were made from flight tests of a blunt and a sharp cone having an apex angle of 50° for Mach numbers up to 4.7 and 4.0, respectively. Reynolds number based on diameter varied from 19.6×10^6 to 32.1×10^6 for the blunt cone, and 18.3×10^6 to 28.4×10^6 for the sharp cone.

Transition occurred at a local Reynolds number from 1×10^6 to 2×10^6 for both models. Momentum transition Reynolds numbers of about 350 were calculated for the blunt cone. Turbulent heat transfer on the sharp cone was approximately 30 percent higher than that on the blunt cone. Heat-transfer data agreed with the theory once transition was determined. Surface roughness for both models was approximately 25 rms microinches.

INDEX HEADINGS

Flow, Viscous	1.1.3
Heating, Aerodynamic	1.1.4.1
Heat Transfer, Aerodynamic	1.1.4.2

[redacted]

NACA RM L57D04

NATIONAL ADVISORY COMMITTEE FOR AERONAUTICS

RESEARCH MEMORANDUM

BOUNDARY-LAYER-TRANSITION AND HEAT-TRANSFER MEASUREMENTS FROM FLIGHT TESTS OF BLUNT AND SHARP 50° CONES AT MACH NUMBERS FROM 1.7 TO 4.7

By Leo T. Chauvin and Katherine C. Speegle

SUMMARY

Boundary-layer-transition and heat-transfer measurements were obtained from flight tests of blunt and sharp cones having apex angles of 50°. The test Mach number range was from 1.7 to 4.7, corresponding to free-stream Reynolds numbers, based on cone base diameter, of 18.3×10^6 and 32.1×10^6, respectively. Transition on both models occurred at a local Reynolds number of 1×10^6 to 2×10^6 based on distance from the stagnation point. Transition Reynolds numbers based on momentum thickness were between 320 and 380 for the blunt cone. The model surface roughness was 25 rms microinches or greater. Turbulent heat transfer to the conical surface of the blunt cone at a Mach number of 4 was 30 percent less than that to the surface of the sharp cone.

Available theories predicted heat-transfer coefficients reasonably well for the fully laminar or turbulent flow conditions.

INTRODUCTION

The National Advisory Committee for Aeronautics is conducting investigations to determine the aerodynamic-heating characteristics of blunt noses. Presented herein are the results of flight tests made by the Langley Pilotless Aircraft Research Division (at its testing station at Wallops Island, Va.) for two noses: a sharp cone and a cone which was blunted to have a ratio of nose radius to base radius of 0.5. Each cone had an apex angle of 50° and a diameter of approximately 1.5 feet. Heat-transfer and transition data are presented for Mach numbers up to 4 and Reynolds numbers based on diameter up to 28.3×10^6 for the sharp cone and for Mach numbers up to 4.7 and Reynolds numbers based on diameter up to 32.1×10^6 for the blunt cone.

Preliminary results from the test of the blunt cone were reported in reference 1.

SYMBOLS

M	Mach number
V	velocity, ft/sec
V_c	velocity of sound, ft/sec
T	temperature, $^{\circ}R$
ρ	density, slugs/cu ft
H	altitude, ft
C_p	pressure coefficient, $\frac{p_l - p_\infty}{0.7 P_\infty M_\infty^2}$
η_r	recovery factor
R	Reynolds number
N_{St}	Stanton number, $\frac{h}{c_p \rho V}$
h	heat-transfer coefficient, Btu/(sec)(sq ft)($^{\circ}R$)
c_p	specific heat, Btu/slug-$^{\circ}R$
τ	thickness, ft
x	distance along surface of body from stagnation point
t	time, sec
g	gravitational acceleration
R_θ	Reynolds number based on momentum thickness
$R_{\theta,T}$	transition Reynolds number based on momentum thickness

[redacted]

N_{Pr} Prandtl number

c_f local skin-friction coefficient

Subscripts:

∞ free stream

l outside boundary layer

w pertaining to wall

aw adiabatic wall

so stagnation

MODELS, INSTRUMENTATION, AND FLIGHT TESTS

Models

Model A.- The general configuration of the blunt cone (designated model A) is shown by the photograph of figure 1(a) and the sketch of figure 1(b). The test nose was mounted on the forward end of an M5 JATO rocket motor which was stabilized by four fins equally spaced about the rearward end of the rocket motor. The test nose was constructed from Inconel approximately 0.031 inch thick. The exterior surface was furnace oxidized to stabilize the emissivity. Surface roughness, as measured by a Physicists Research Co. Profilometer prior to the oxidizing process, was approximately 25 rms microinches. Oxidation of the surface may have increased the roughness still further.

Model B.- The general configuration of the sharp cone (designated model B) is shown by the photograph of figure 2(a) and the sketch of figure 2(b). Except for the nose shape, the model was similar to model A. The surface of this model was also oxidized and had about the same surface roughness as model A. Details of the nose tip are given in figure 2(b). A photograph of model A in launching position is shown in figure 3.

Instrumentation

Model A.- An NACA nine-channel telemeter was carried in the nose portion of the model and transmitted wall temperatures, pressures, and longitudinal accelerations to ground receiving stations. The 12 temperature pickups were commutated every 0.25 second. The no. 30 gage

[redacted]

chromel-alumel thermocouples were welded in a ray to the inner surface of the skin at the stations shown in figure 1(b). Six of the channels transmitted continuous readings of pressure at the stations shown in figure 1(b). The pressure orifices were made by welding monel tubing (outer diameter, 0.060 inch; inner diameter, 0.040 inch) to the skin. The instrumentation had a time-lag constant of about 0.007 second, which was sufficiently small to allow measurement of the rapid pressure changes obtained during the accelerating flight. The pressure cells were connected to read differential pressures referenced to pickup 5. The absolute pressure for all stations could be derived by summing the pressure differences between stations with respect to station P_5 or by utilizing existing pressure measurements for hemispheres to calculate the absolute pressure for station P_1 located on the hemisphere and referencing the other measurements to it.

Model B.- The instrumentation for model B was the same as that for model A, except that only one pressure measurement, which proved to be defective, was made. The locations of the thermocouples are shown in figure 2(b).

General.- Trajectory data were obtained by using an NACA modified SCR-584 position radar. Atmospheric and wind conditions were measured by means of radiosondes launched near the time of flight and tracked by a Rawin set AN/GMD-1A. Model velocity was obtained from CW doppler radar and from the integration of telemetered longitudinal accelerations. Atmospheric conditions as obtained from the radiosonde measurements are presented in figures 4(a) and (b) for models A and B, respectively. Figures 4(a) and (b) also present the altitude time history of the model.

Flight Tests

Models A and B utilized a two-stage propulsion system consisting of an M6 JATO "Honest John" booster, which propelled the model to a Mach number of 2.2, and an M5 JATO "Nike" sustainer motor, which further accelerated the model. A 2-second coast period occurred between booster burnout and sustainer ignition. Indications are that the stabilizing fins of both models failed because of aerodynamic heating shortly before burnout of the second stage. The failures have since been studied by simulating the flight heat input to the outboard portion of a duplicate fin in a high-temperature, M = 2 free jet. Preliminary results of this study are presented in reference 2.

Despite the fin failure, undisturbed heating data were obtained for a Mach number range from 2.5 to 4.7 for model A and from 1.67 to 3.94 for model B. The variation of Mach number and free-stream Reynolds number per foot is presented as a function of time in figures 5(a) and (b)

for models A and B, respectively. Both models followed essentially the same trajectory up to the time of failure. Both models were launched at an angle of 55°.

DATA REDUCTION

From measured wall temperatures, flight conditions and measured (model A) or estimated (model B) pressures, Stanton numbers were obtained by using the following relation

$$N_{St}\left(c_p \rho V\right)_l = \frac{\left(\tau \rho c_p\right)_w}{T_{aw} - T_w} \frac{dT_w}{dt}$$

Heat losses due to conduction and radiation were found to be negligible when compared with the heat transfer to the nose caused by convection. The skin thickness τ_w was measured and the density ρ_w of the Inconel was known. The specific heat of Inconel $c_{p,w}$ is given in reference 3 as a function of temperature. The adiabatic wall temperature T_{aw} was computed from the relation

$$T_{aw} = \eta_r\left(T_{so} - T_l\right) + T_l$$

where the recovery factor η_r was determined from the usual turbulent relation $\eta_r = N_{Pr}^{1/3}$ with Prandtl number evaluated at the wall temperature. It is realized that a recovery factor equal to $N_{Pr}^{1/3}$ is not accurate at the stagnation point and for the regions of laminar flow. However, this approximation to the true recovery factor results in an error of less than 2 percent for conditions of this test. A temperature gradient existed across the 0.032-inch Inconel skin. This gradient was neglected in determining the Stanton numbers presented herein. The effect of neglecting the gradient has been estimated for model A. The maximum estimated error in Stanton number was from 10 to 15 percent for stations 6 and 7 and 5 percent for the other stations.

The local conditions for model A were determined by using pressure measurements and normal shock relations (ref. 4). Local conditions for model B were determined from cone theory (ref. 5).

[redacted]

RESULTS AND DISCUSSION

Model A

Pressure measurements.- Pressures were measured on the nose at the locations shown in figure 1(b). The measurements expressed as pressure coefficients are shown in figure 6 plotted as a function of the distance along the nose from the stagnation point. The experimental data are compared with pressure calculated by modified Newtonian theory. The theory is seen to be in better agreement with experimental data at the higher Mach numbers. The experimental data also show an adverse pressure gradient in the region of the hemisphere-cone juncture which is not predicted by theory.

Temperature measurements.- The variation of measured wall temperature with time is presented in figure 7 for all stations except station 11, for which no data were obtained because of thermocouple failure. Temperature data are presented to a flight time of 9.5 seconds, at which time model failure occurred. Heat-transfer data were reduced from these skin temperatures to 9.30 seconds, at which time the Mach number was 4.7. Temperatures plotted as a function of distance from the stagnation point to the measuring station are presented in figure 8 for various Mach numbers. Transition is indicated by the rapid increase in temperature at about 1.5 inches (approximately 20°) from the stagnation point.

Heat-transfer coefficients and transition.- Heat-transfer coefficients are presented in figure 9 for various conditions of Mach number and Reynolds number. The data are presented in the form of local Stanton number $\left(\frac{h}{c_p \rho V}\right)_l$ varying with distance from the stagnation point. The local Reynolds number based on distance from the stagnation point and conditions just outside the boundary layer and the ratio T_w/T_l are also presented as a function of distance from the stagnation point.

The data for the stagnation point which are also presented in the form of Stanton number are based on conditions behind the normal shock.

In general, the data measured at the stagnation point and at points in the laminar region close to the stagnation point are in fair agreement with the theory of references 5 and 6, respectively. The data show a rapid rise in heat transfer at about 1.5 inches or 20° from the stagnation point. This rise is attributed to transition from laminar to turbulent flow. Transition occurs between local Reynolds numbers of 1×10^6 and 2×10^6.

The turbulent values of Stanton number on the conical section of the nose are seen to be in fair agreement with the turbulent flat plate theory of reference 7, with a Reynolds number based on length from the stagnation point and the assumption that $N_{St} = 0.5c_f$.

Figure 10 presents the Reynolds number of transition based on the calculated momentum thickness (ref. 8) as a function of distance from the stagnation point. For the flight condition of model A, the transition point was fixed at approximately 0.14 foot from the stagnation point or about 22°. The two points represent the small difference in the momentum Reynolds number for Mach numbers ranging from 2.5 to 4.7. Shown also in the figure are the measurements of transition obtained from a flight test of another blunt cone (ref. 9) where the flight conditions were similar to those of the present investigation except that the model had a ratio of nose radius to base radius of 0.74, and the surface was polished to a surface roughness of 3 to 5 microinches. Figure 10 shows that for model A, for which the roughness was approximately 25 rms microinches, transition occurred at a low transition Reynolds number $R_\theta \approx 350$, while for the reference model transition varied from $R_\theta = 800$ to 2,180. It is conjectured that the surface roughness of 25 microinches resulted in tripping the relatively thin boundary layer associated with the blunt nose at this low Reynolds number.

Model B

Temperature measurements.- The variation of measured wall temperatures with time is presented in figure 11. No data are shown for thermocouples 6, 8, and 12, which failed early in the flight. Temperature data are presented to a flight time of 9.4 seconds, at which time model failure occurred. Heat-transfer data were reduced from these measurements to 9.4 seconds, at which time the Mach number was 3.97.

Figure 12 presents the skin temperatures as a function of distance from the nose tip for various Mach numbers. Transition is again indicated to have taken place near the nose tip.

Heat-transfer coefficients and transition.- Heat-transfer coefficients $N_{St} = \left(\frac{h}{c_p \rho V}\right)_l$, along with local Reynolds number and ratio T_w/T_l, are presented in figure 13 as a function of distance from the stagnation point. Sufficient laminar data were not acquired to warrant a conclusion as to the adequacy of laminar theory. Transition, as indicated by the large increase in Stanton number, is seen to occur between 1 and 2 inches from the nose tip. The local Reynolds numbers of transition are about

[redacted]

1×10^6 to 2×10^6 or the same as for the blunt cone. It is again pointed out that the surface roughness of this model was 25 microinches or greater.

The turbulent heat-transfer coefficients are seen to be generally in good agreement with the cone theory of Van Driest (ref. 10) with a Reynolds number based on length from the stagnation point and the assumption that $N_{St} = 0.5c_f$. Heat-transfer measurement from nose tip was not presented inasmuch as some uncertainty existed as to the exact depth of the thermocouple installation.

Comparison of turbulent heat-transfer coefficients for blunt and sharp cones.- Figure 14 presents a comparison of the turbulent heat-transfer coefficients measured on the blunt and sharp cones. It is seen that, for about the same values of free-stream Reynolds number per foot and for cases in which transition occurred close to the stagnation point for both models, the heating to both noses on the conical surface is about the same at a Mach number of 2.5; at a Mach number of 4, however, the heating to the blunt cone is approximately 30 percent less than that to the sharp cone. The average heat-transfer coefficient obtained by integrating the local heat-transfer coefficient was approximately 20 percent lower for the blunt cone at a Mach number of 4 and about the same for both cones at a Mach number of 2.5.

CONCLUDING REMARKS

Flight tests have been made of blunt and sharp cones having apex angles of 50° at Mach numbers up to 4.7 and 4, respectively. Boundary-layer transition occurred at a local Reynolds number of 1×10^6 to 2×10^6 based on length from the stagnation point on both nose shapes. This Reynolds number corresponds to a value of about 350 based on calculated momentum thickness for the blunt cone. At a Mach number of 4, the turbulent heat-transfer coefficient to the conical surface was 30 percent less on the blunted cone. Heat-transfer coefficients for both models could be predicted reasonably well by available theory for the fully laminar or turbulent flow conditions.

Langley Aeronautical Laboratory,
National Advisory Committee for Aeronautics,
Langley Field, Va., March 20, 1957.

Leo T. Chauvin
Aeronautical Research Engineer

Katherine C. Speegle
Aeronautical Research Engineer

Approved: Joseph A. Shortal
Joseph A. Shortal
Chief of Pilotless Aircraft Research Division

rwh

[redacted]

REFERENCES

1. Chauvin, Leo T.: Aerodynamic Heating of Aircraft Components. NACA RM L55L19b, 1956.

2. Bland, William M., Jr., and Bressette, Walter E.: Some Effects of Heat Transfer at a Mach Number of 2.0 at Stagnation Temperatures Between 2,310° and 3,500° R on a Magnesium Fin With Several Leading-Edge Modifications. NACA RM L57C14, 1957.

3. Ginnings, Defoe C., and Thomas, Eugenia: The Electrical Resistance and Total Radiant Emittance of Inconel in the Range 0° to 1000° C. NBS Rep. 4111 (NACA Contract S-54-52), Nat. Bur. Standards, May 1955.

4. Ames Research Staff: Equations, Tables, and Charts for Compressible Flow. NACA Rep. 1135, 1953. (Supersedes NACA TN 1428.)

5. Sibulkin, M.: Heat Transfer Near the Forward Stagnation Point of a Body of Revolution. Jour. Aero. Sci. (Readers' Forum), vol. 19, no. 8, Aug. 1952, pp. 570-571.

6. Van Driest, E. R.: The Problem of Aerodynamic Heating. Aero. Eng. Rev., vol. 15, no. 10, Oct. 1956, pp. 26-41.

7. Van Driest, E. R.: The Turbulent Boundary Layer for Compressible Fluids on a Flat Plate With Heat Transfer. Rep. No. AL-997, North American Aviation, Inc., Jan. 27, 1950.

8. Anon.: X-17 Re-Entry Test Vehicle - R-1 Final Flight Report. Rep. No. MSD-1834 (Contract No. AF 04 (645)-7), Lockheed Aircraft Corp., July 17, 1956.

9. Buglia, James J.: Heat Transfer and Boundary-Layer Transition on a Highly Polished Hemisphere-Cone in Free Flight to a Mach Number of 3.14 and Reynolds Number of 24×10^6. NACA RM L57D05, 1957.

10. Van Driest, E. R.: Turbulent Boundary Layer on a Cone in a Supersonic Flow at Zero Angle of Attack. Jour. Aero. Sci., vol. 19, no. 1, Jan. 1952, pp. 55-57, 72.

[redacted]

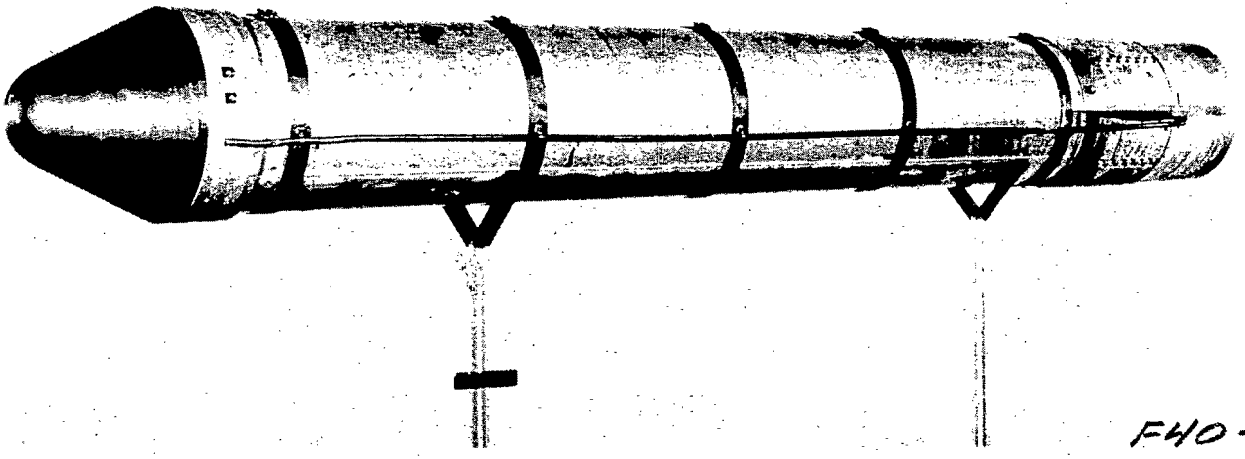

(a) Photograph of model. L-90835

Figure 1.- Blunt-cone configuration, model A.

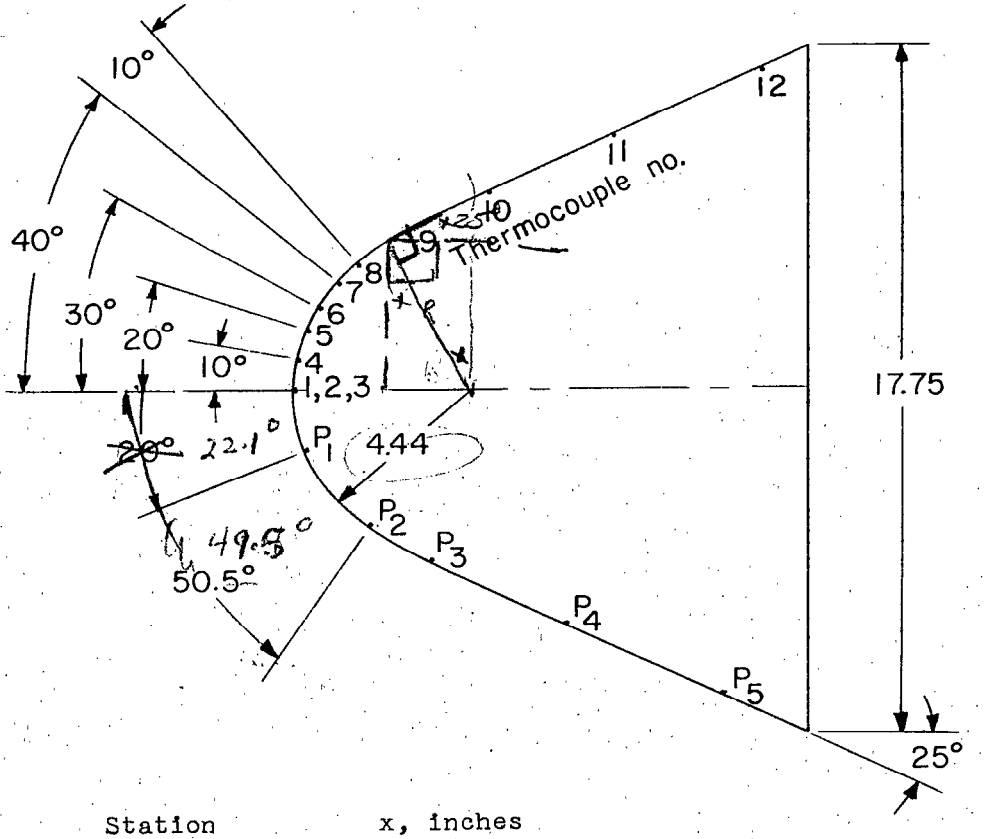

Station	x, inches
Thermocouple	
1,2,3	0, approx.
4	0.75
5	1.50
6	2.32
7	3.10
8	3.87
9	5.90
10	7.65
11	11.08
12	15.15
Pressure	
1	1.72
2	3.84
3	6.02
4	9.65
5	14.15

(b) Sketch of configuration.

Figure 1.- Concluded.

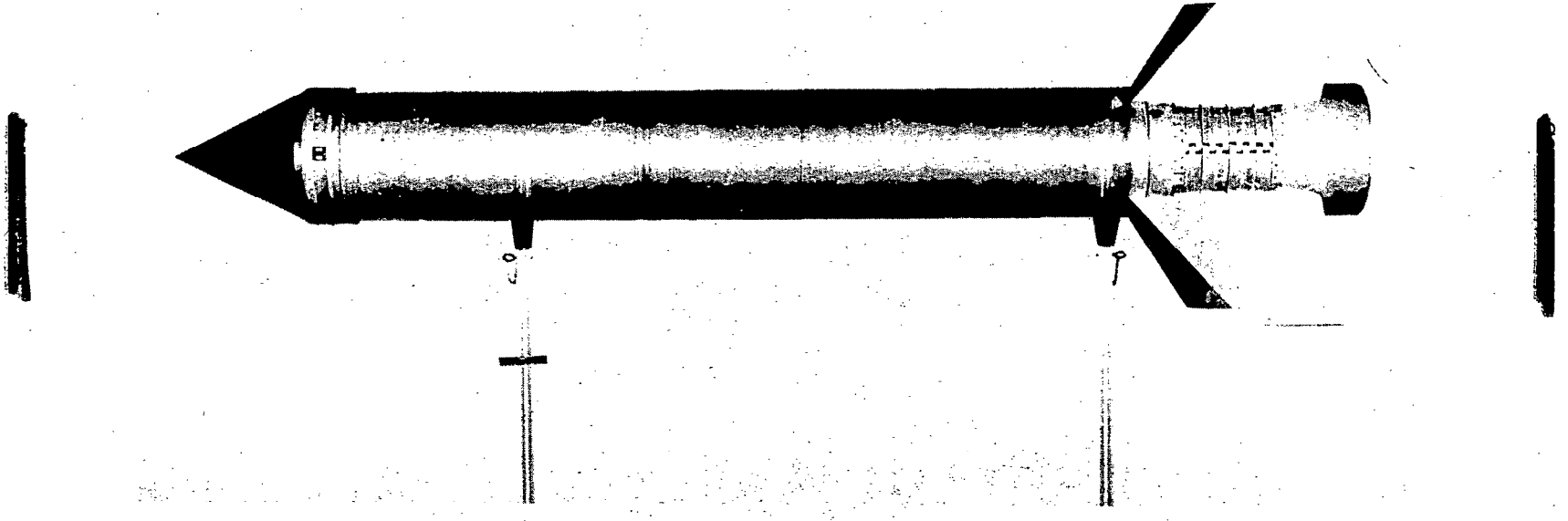

(a) Photograph of model. L-92002

Figure 2.- Sharp-cone configuration, model B.

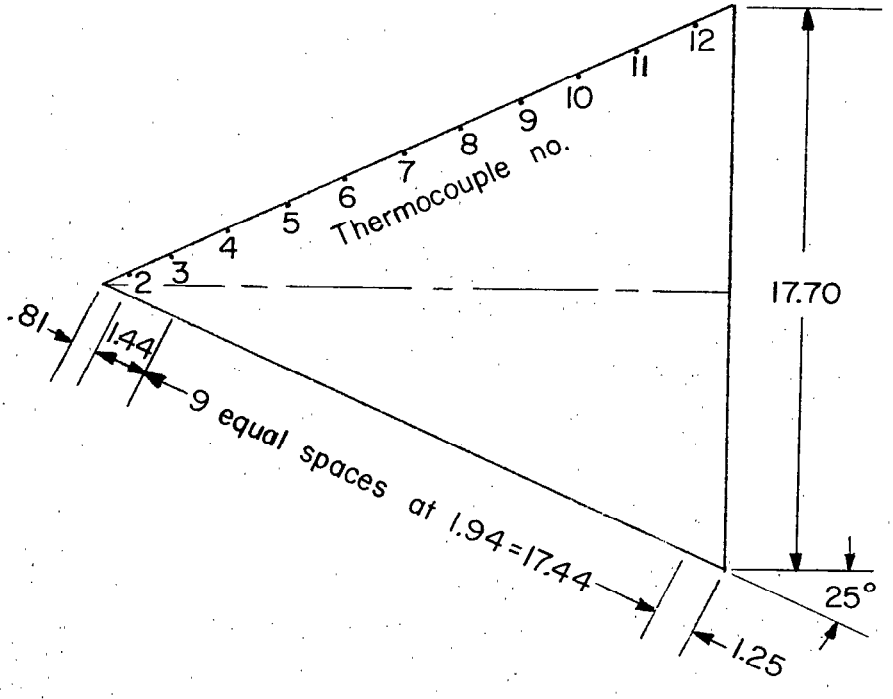

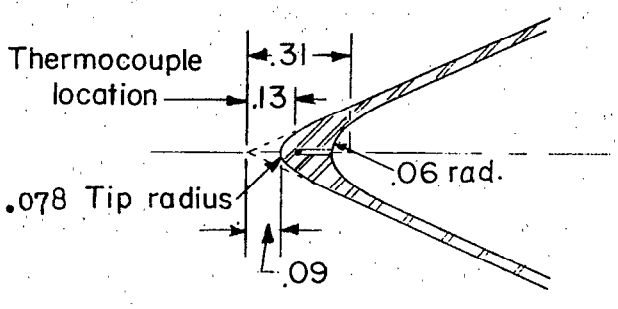

Station	x, inches
1	0
2	0.81
3	2.25
4	4.19
5	6.13
6	8.06
7	10.00
8	11.94
9	13.88
10	15.81
11	17.75
12	19.69

(b) Sketch of configuration.

Figure 2.- Concluded.

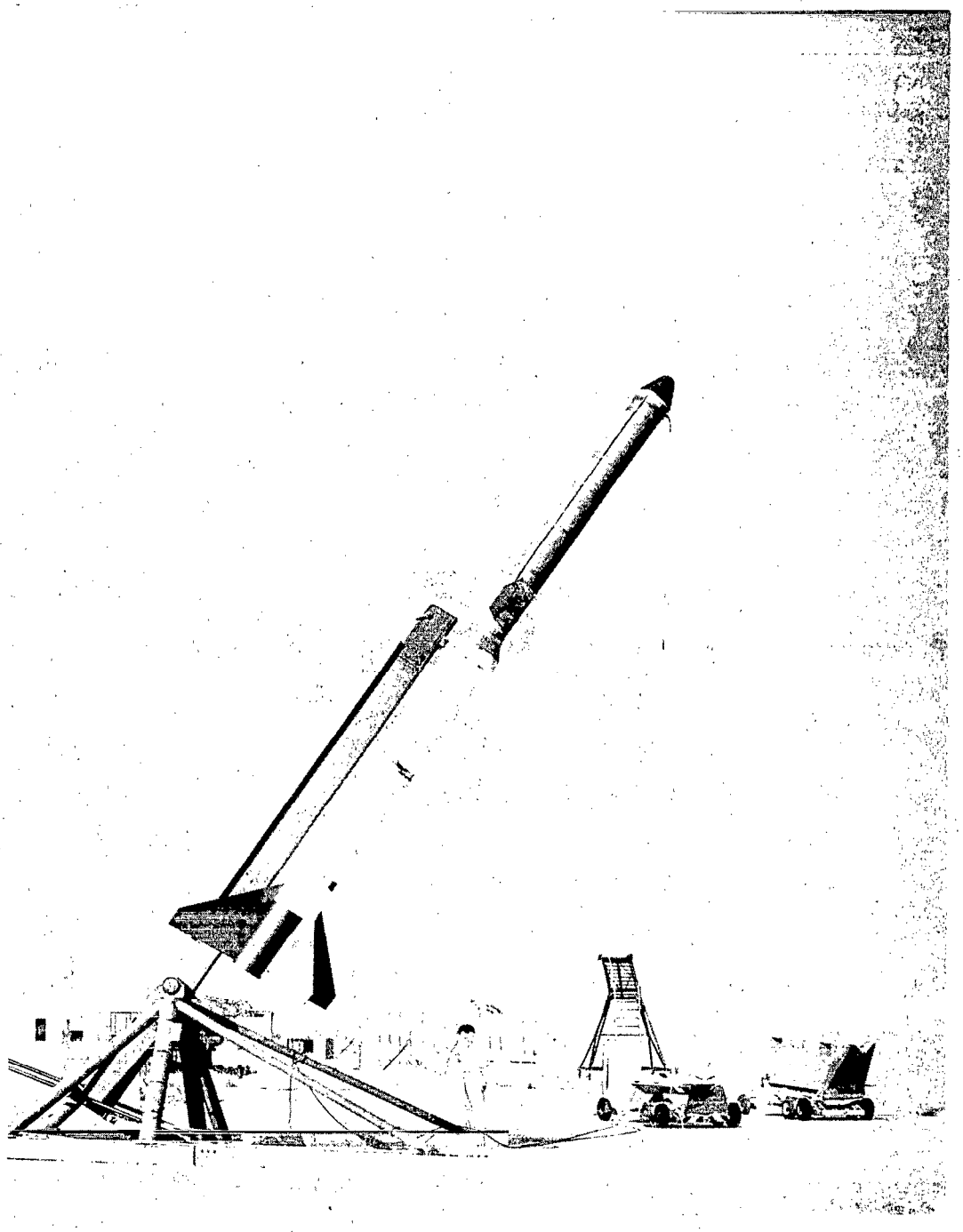

L-90962

Figure 3.- Photograph of model A in launching position.

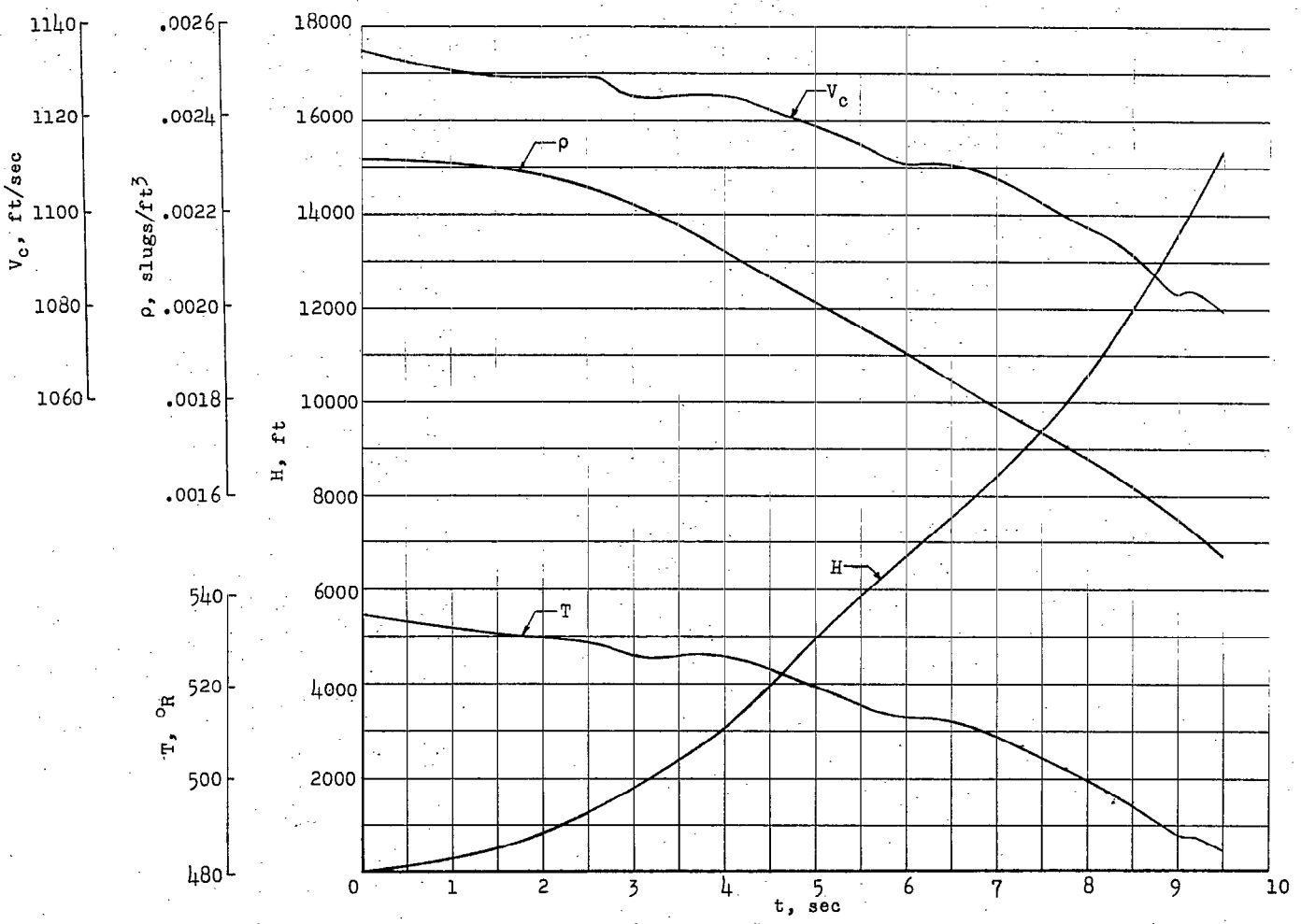

(a) Model A.

Figure 4.- Time histories of atmospheric conditions and altitude.

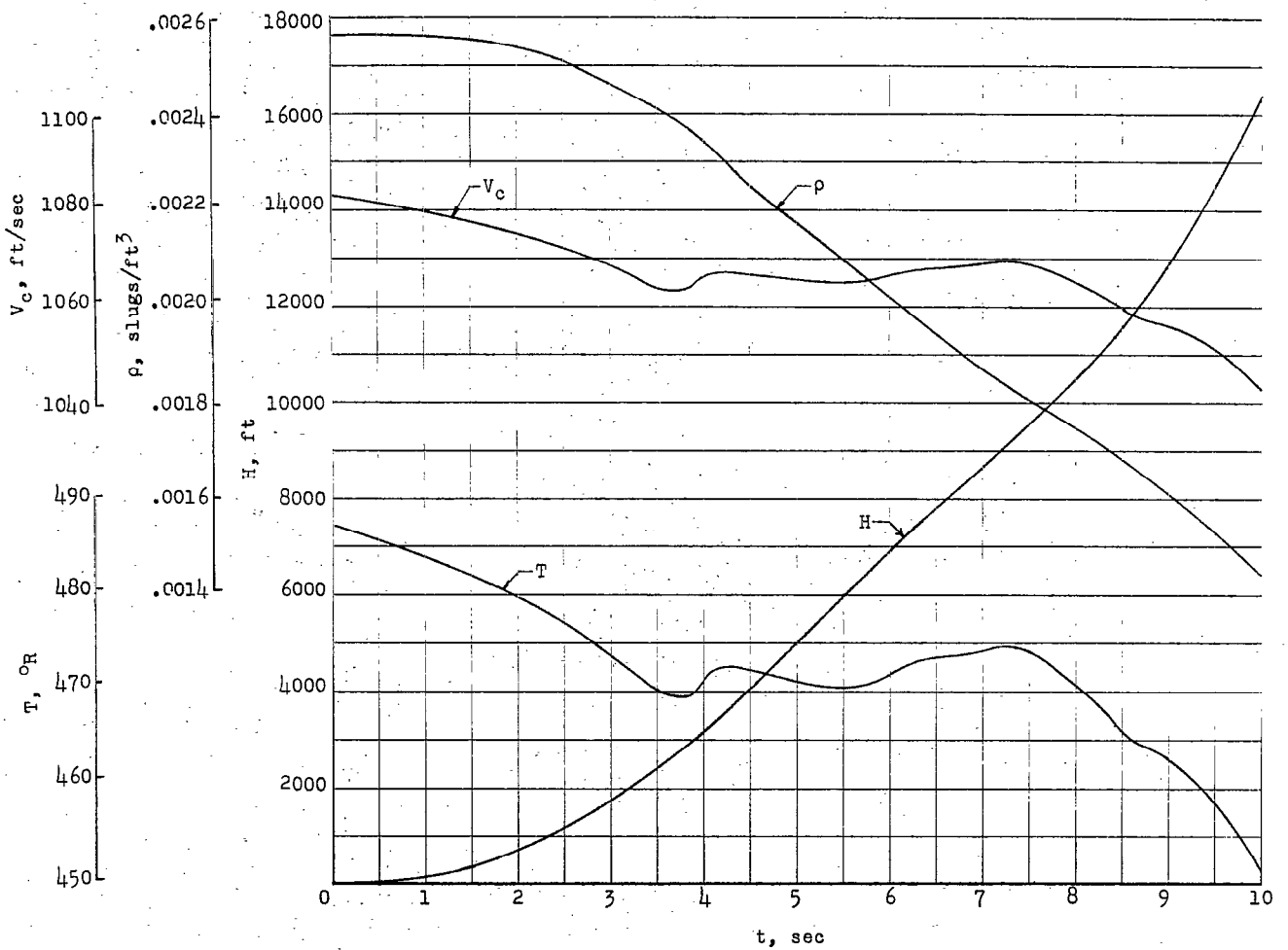

(b) Model B.

Figure 4.- Concluded.

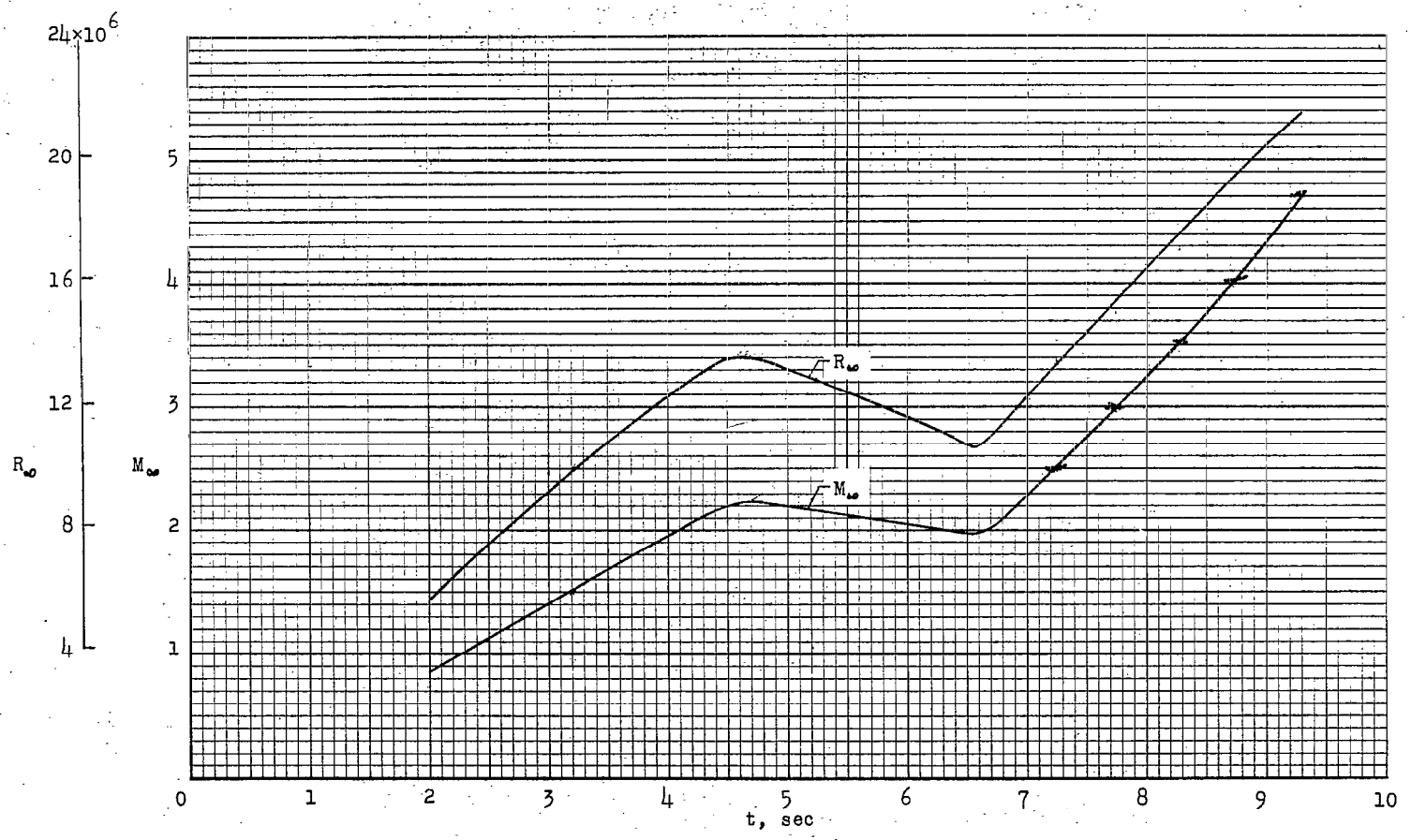

(a) Model A.

Figure 5.- Time histories of Mach number and free-stream Reynolds number per foot.

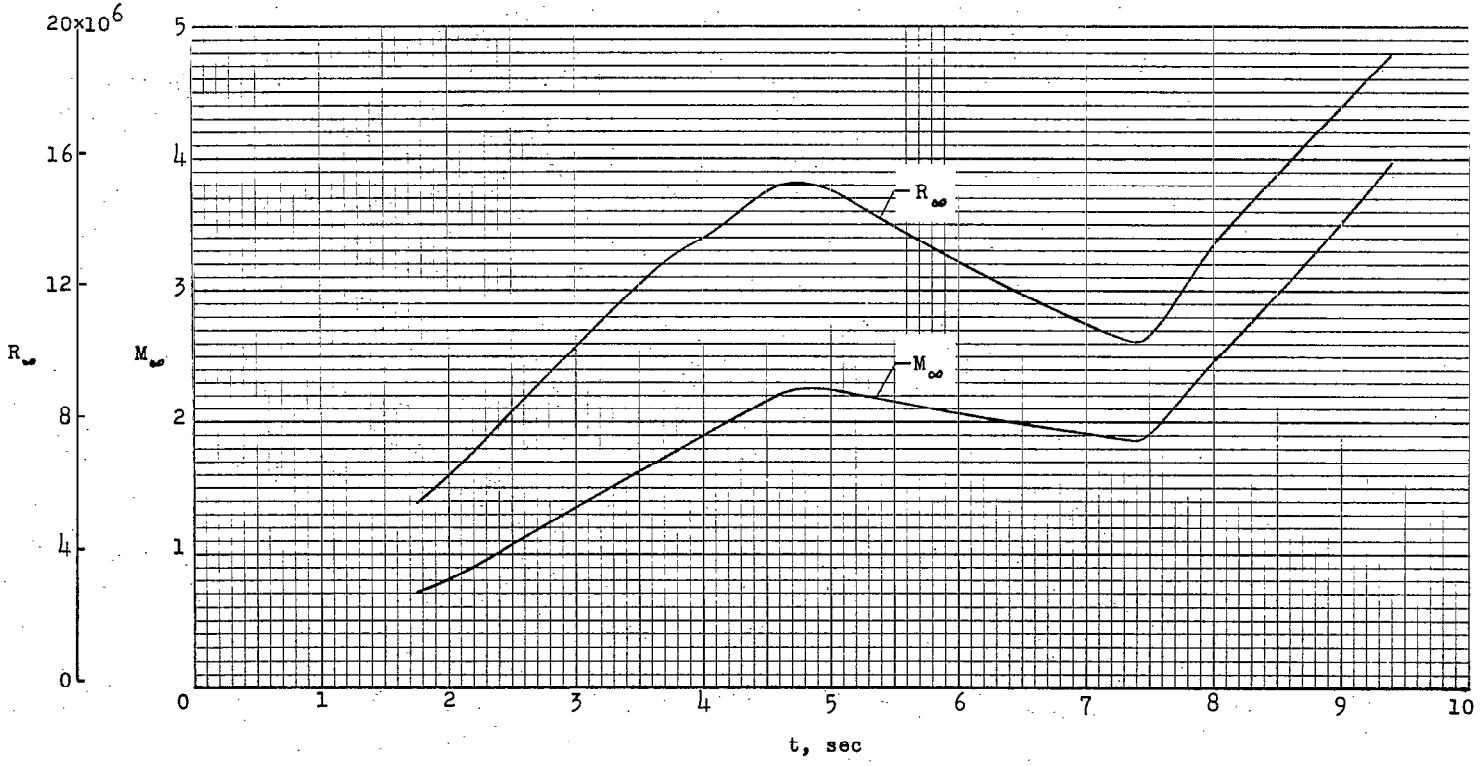

(b) Model B.

Figure 5.- Concluded.

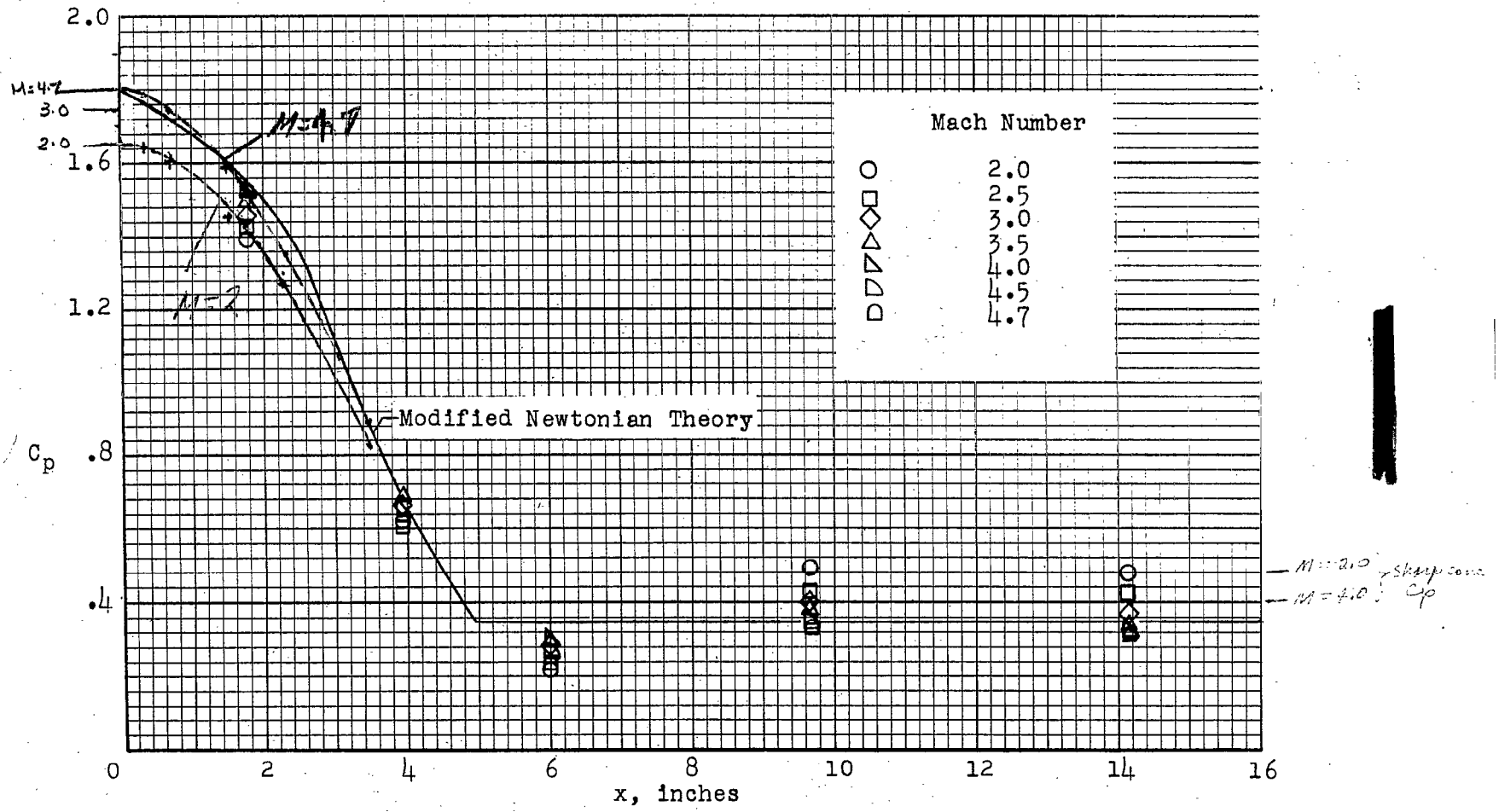

Figure 6.- Measured pressure coefficients for model A.

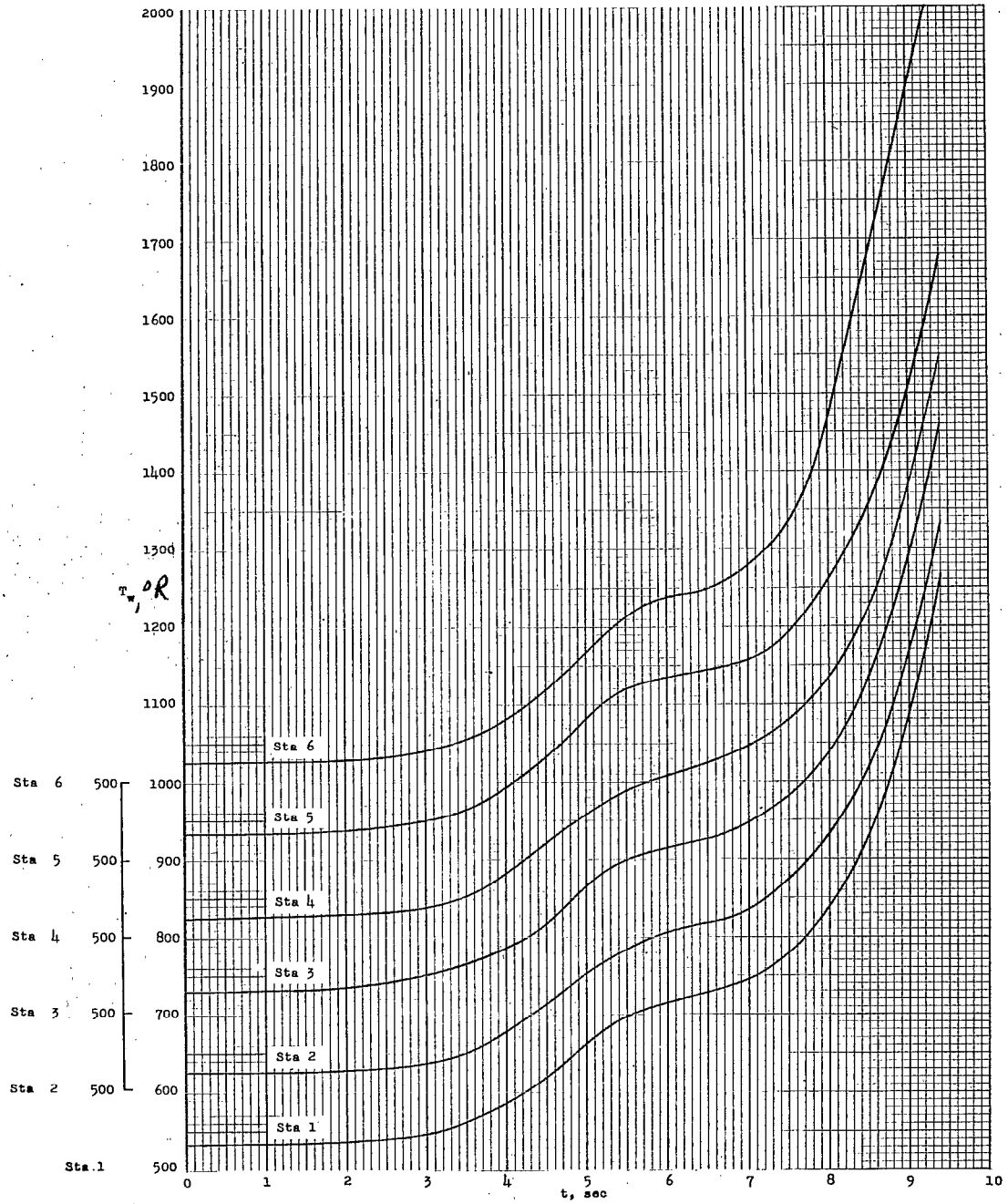

(a) Thermocouple numbers 1 to 6.

Figure 7.- Skin temperature time histories for model A.

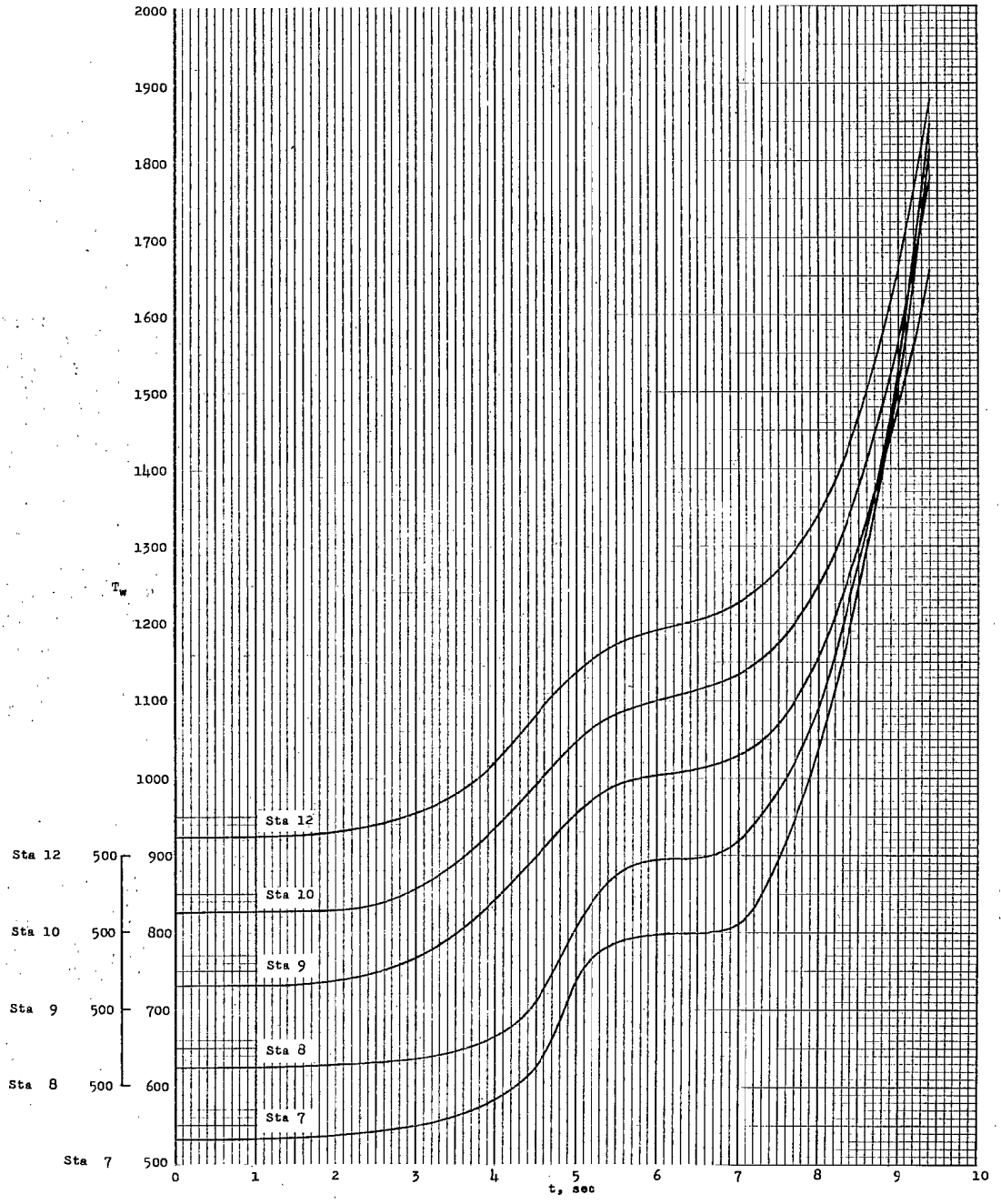

(b) Thermocouple numbers 7 to 10 and 12.

Figure 7.- Concluded.

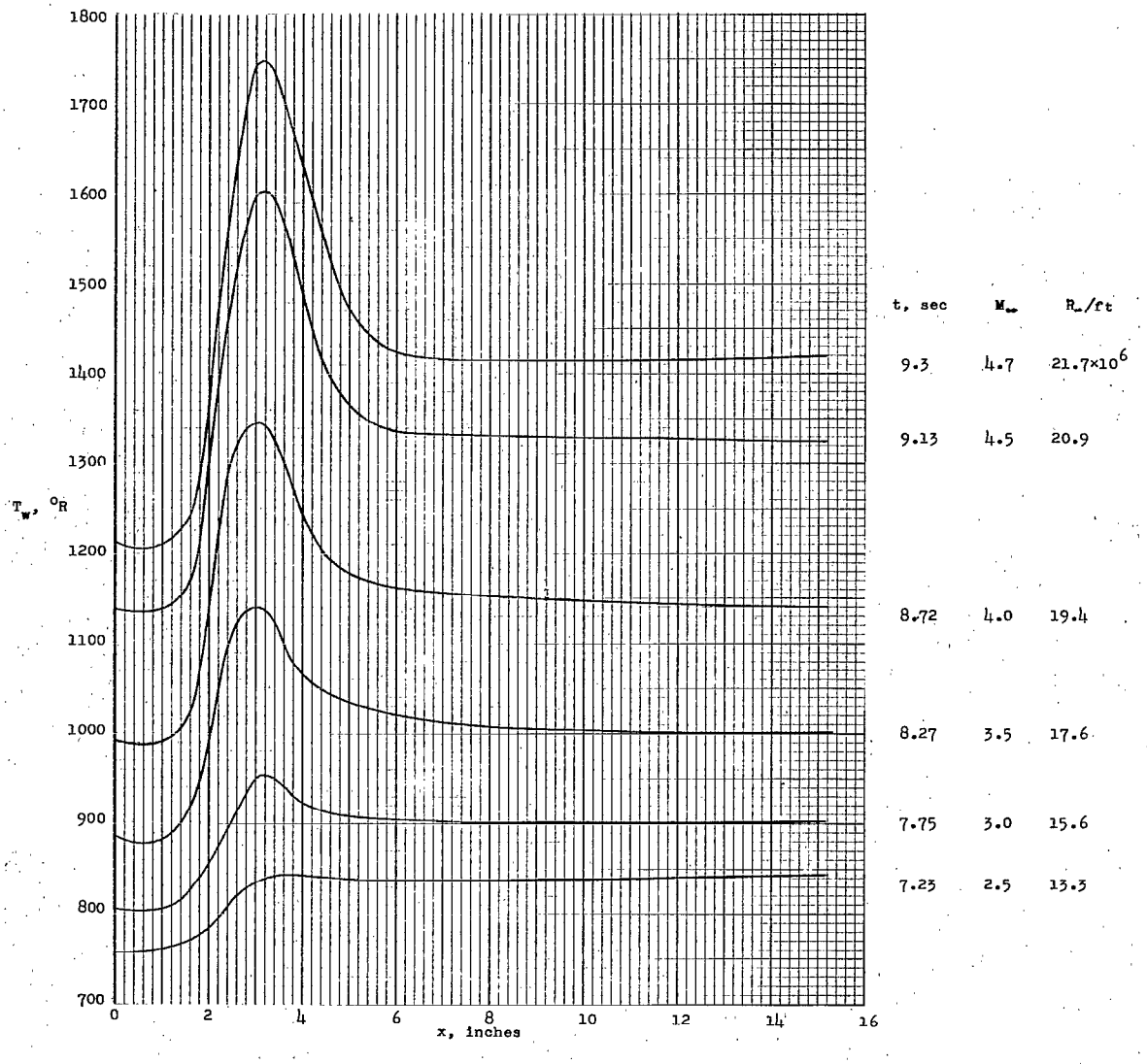

Figure 8.- Skin temperatures along the nose for several Mach numbers. Model A.

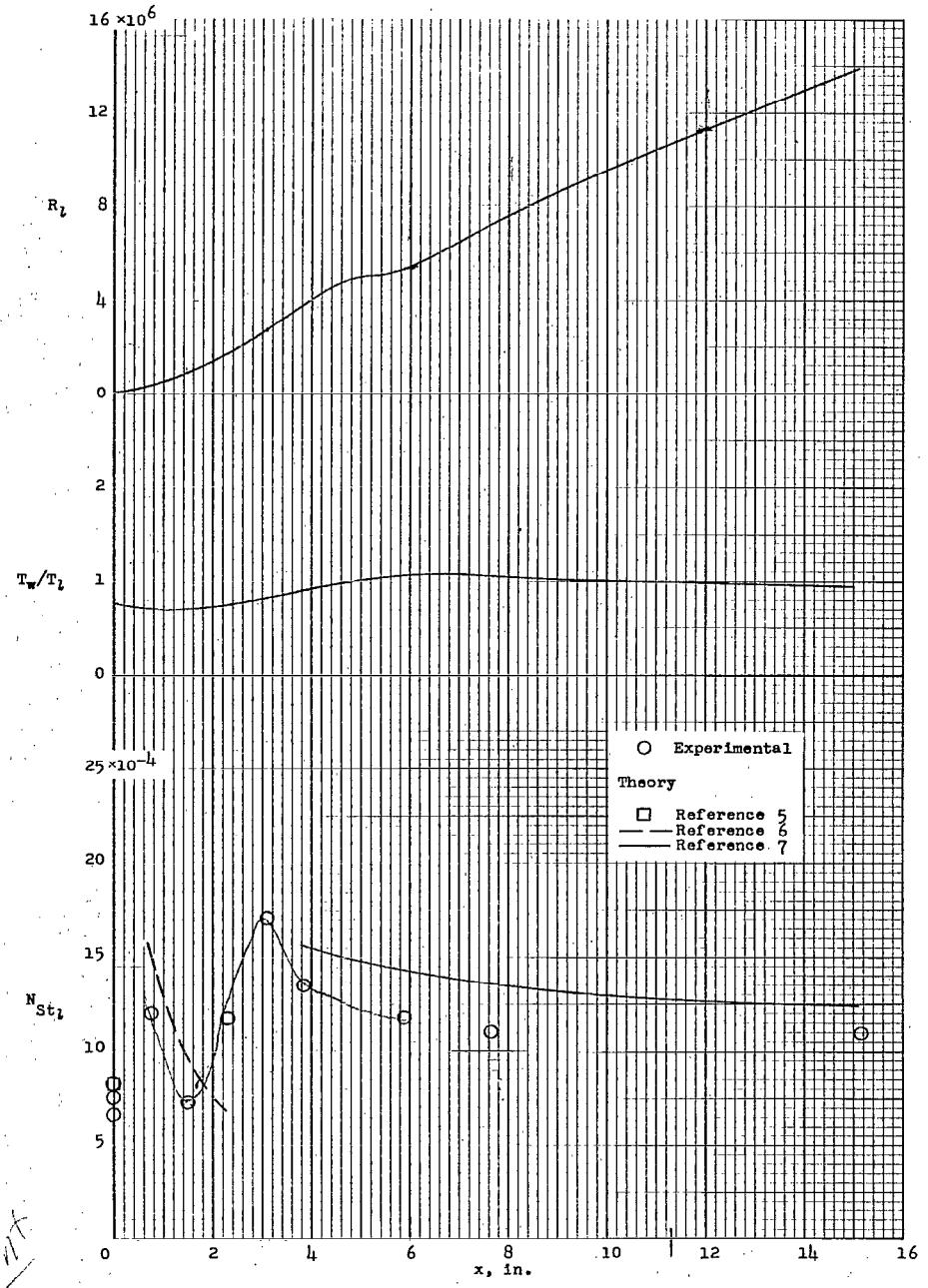

(a) M = 2.5.

Figure 9.- Variation of local Stanton numbers, Reynolds numbers, and ratios of wall temperature to local static temperature along nose for several Mach numbers. Model A.

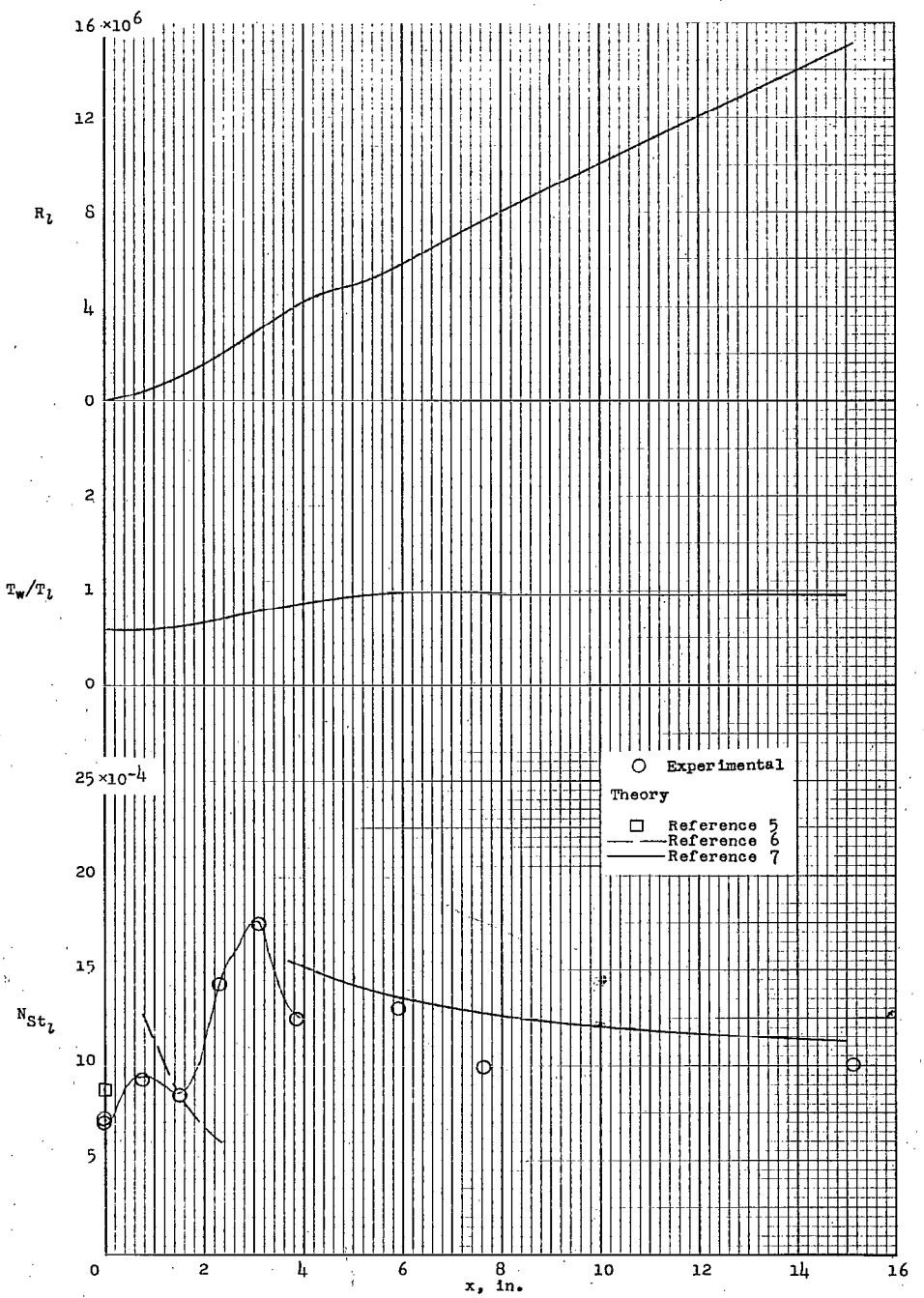

(b) M = 3.0.

Figure 9.- Continued.

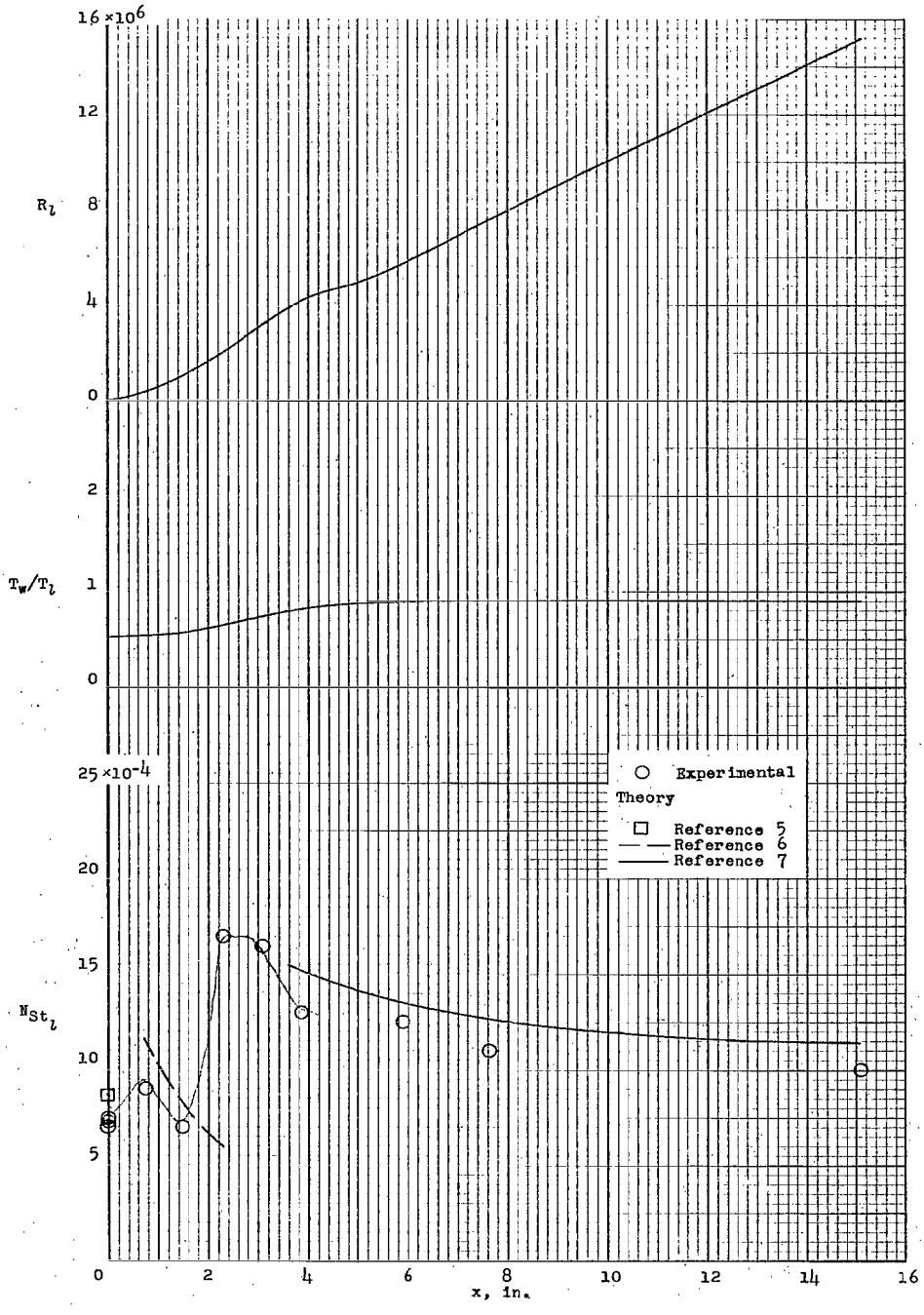

(c) M = 3.5.

Figure 9.- Continued.

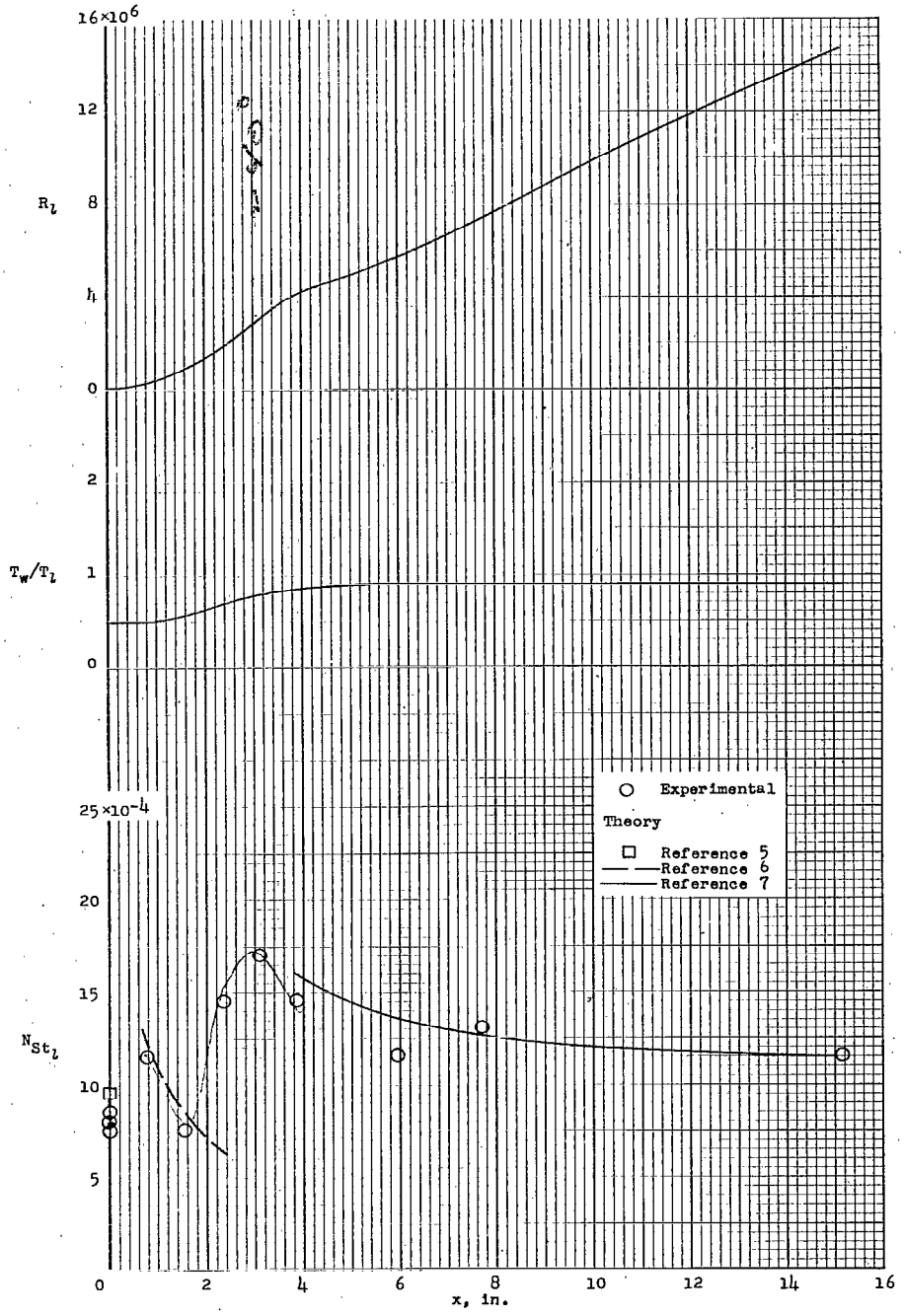

(d) M = 4.0.

Figure 9.- Continued.

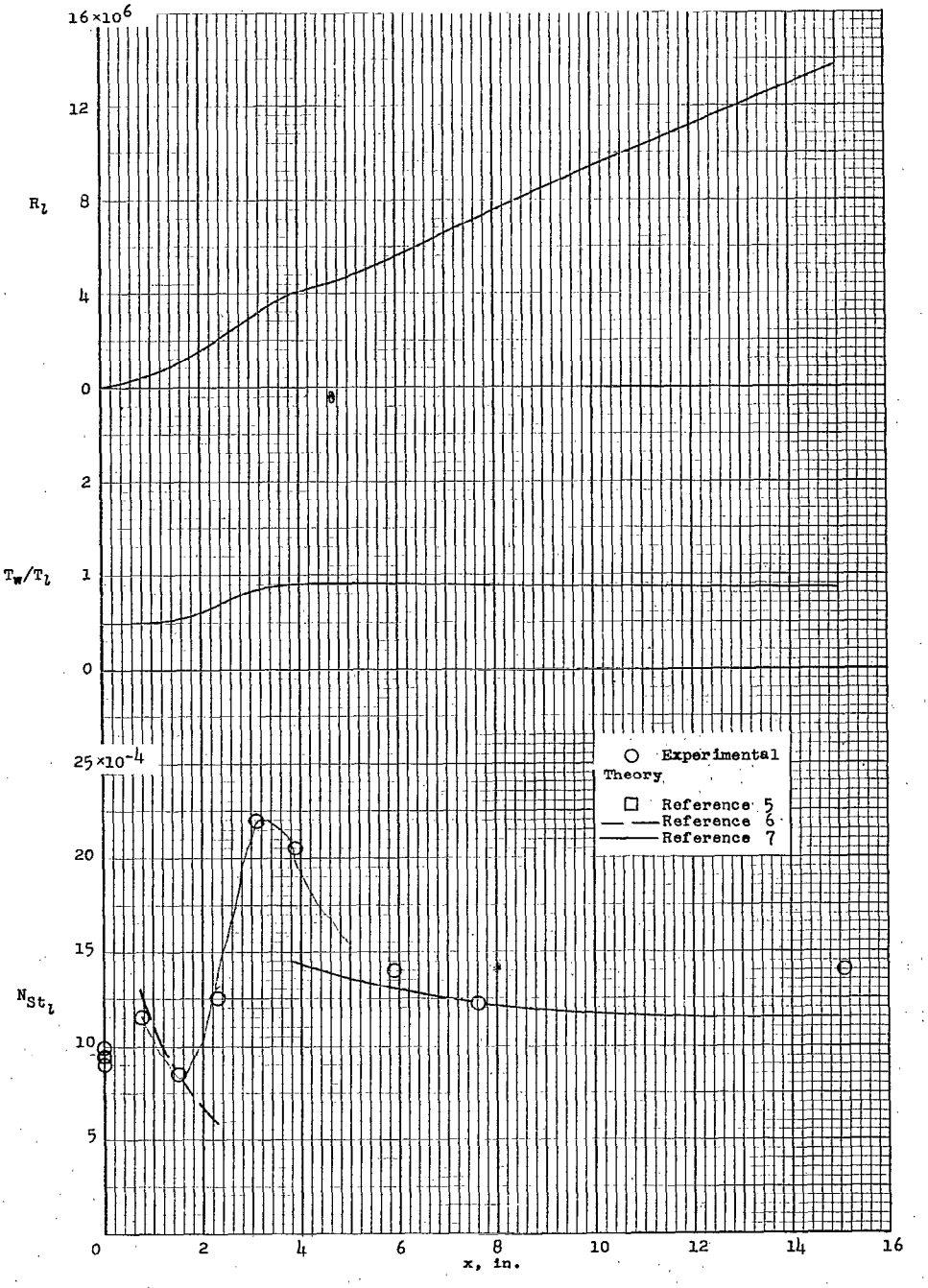

(e) M = 4.7.

Figure 9.- Concluded.

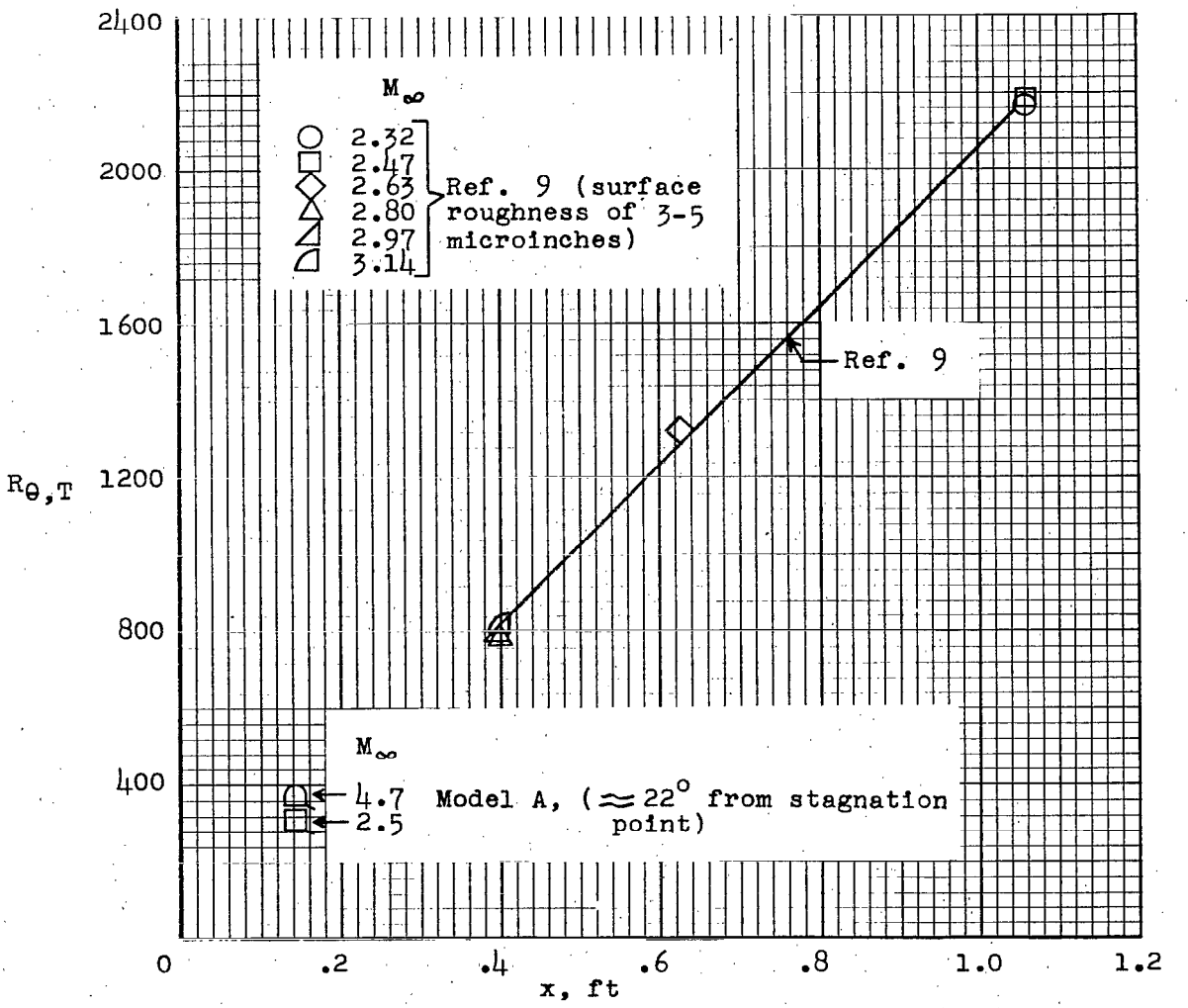

Figure 10.- Comparison of transition Reynolds numbers (based on momentum thickness) for a highly polished hemisphere-cone and model A.

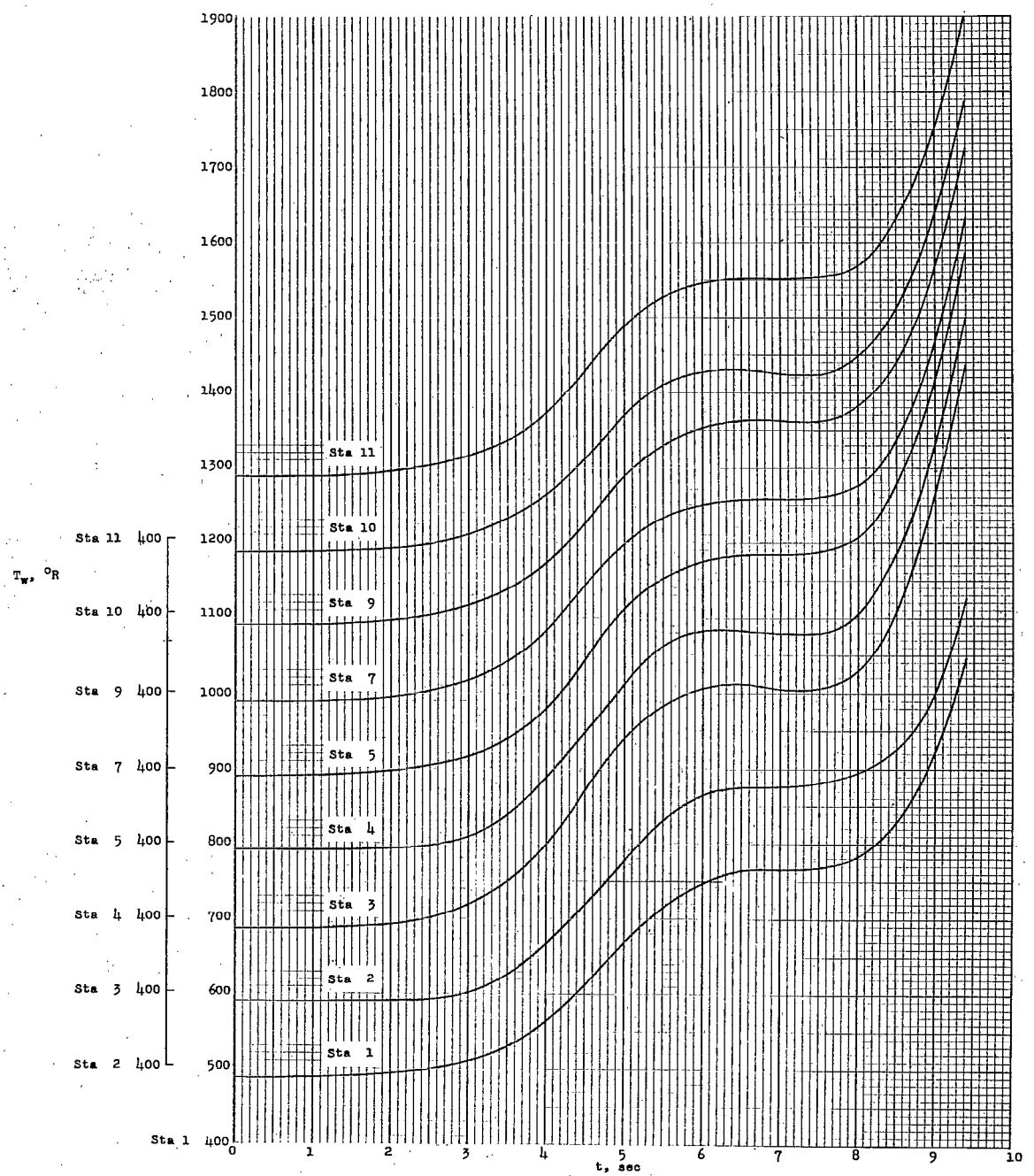

Figure 11.- Wall-temperature time histories for model B.

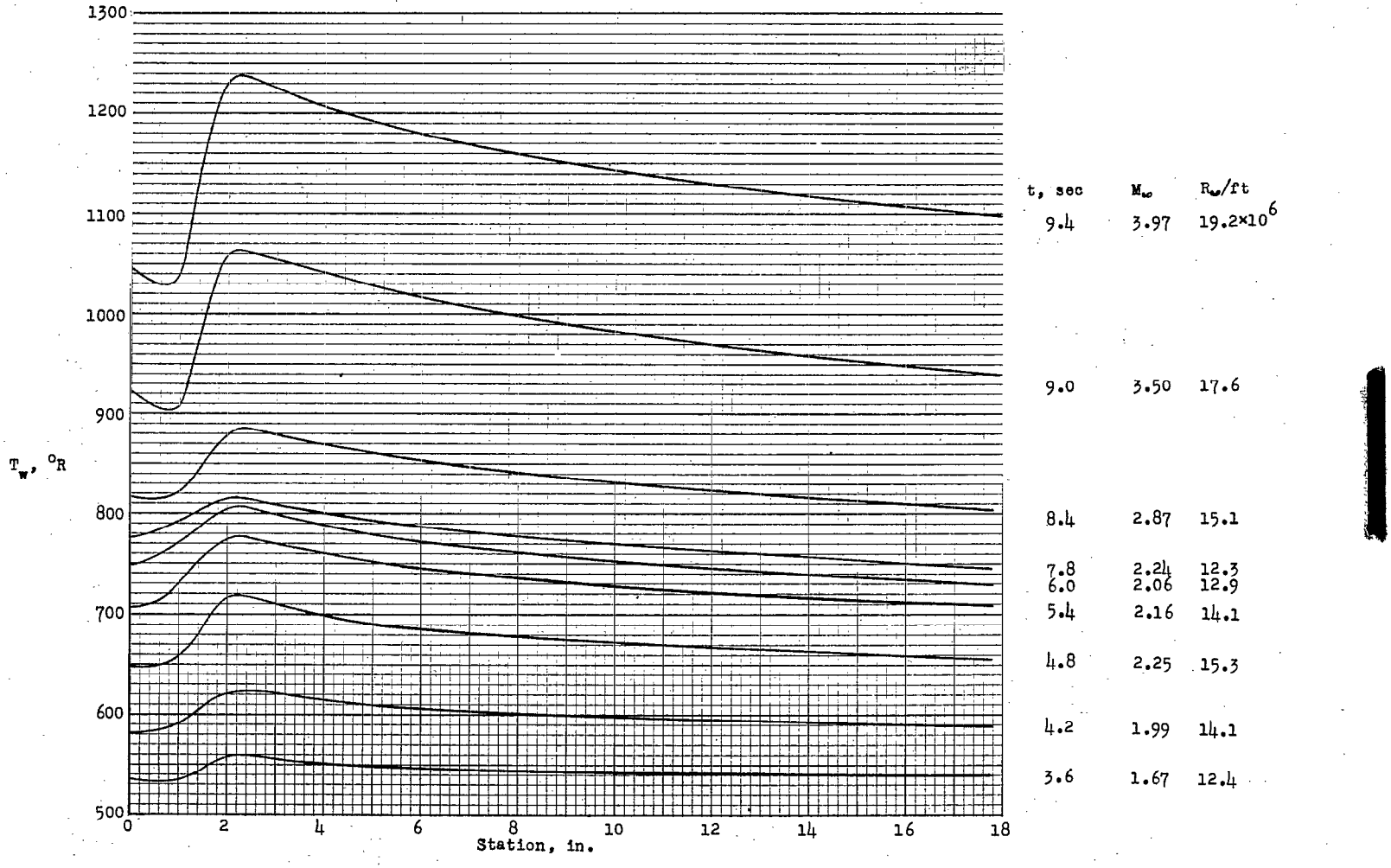

Figure 12.- Wall-temperatures along nose for several Mach numbers.

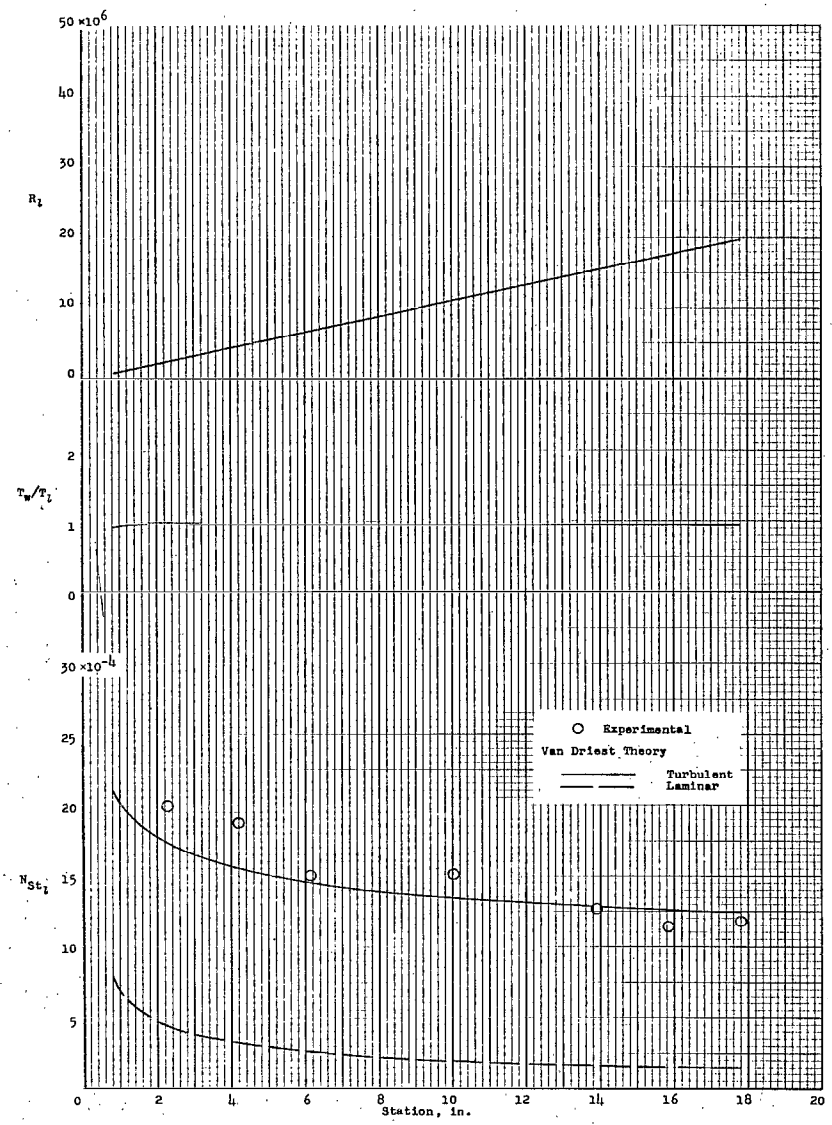

(a) $t = 3.6$ seconds; $M_\infty = 1.67$.

Figure 13.- Variation of local Stanton numbers, Reynolds numbers, and ratios of wall temperature to local static temperature along nose for several Mach numbers. Model B.

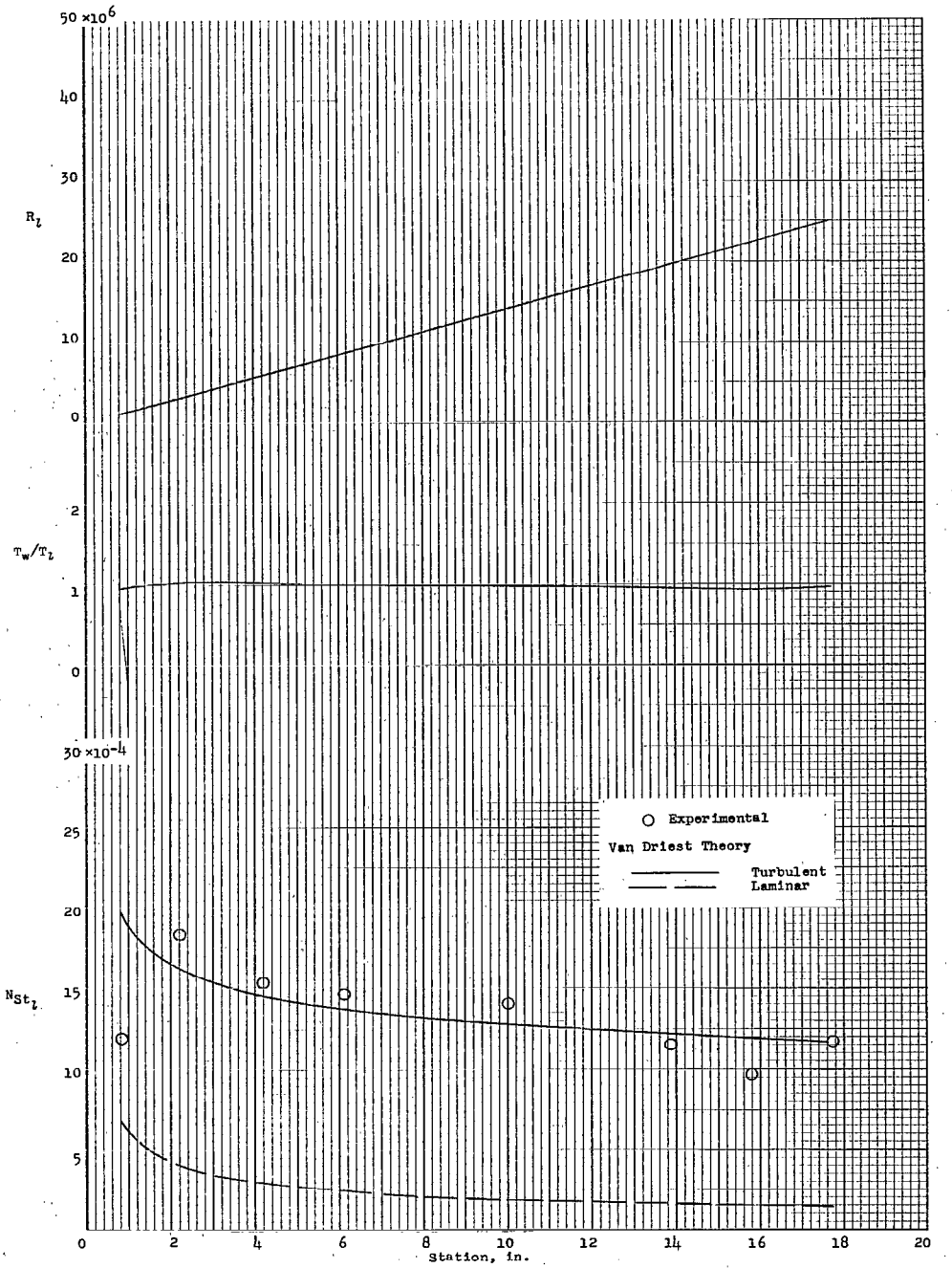

(b) t = 4.2 seconds; M_∞ = 1.99.

Figure 13.- Continued.

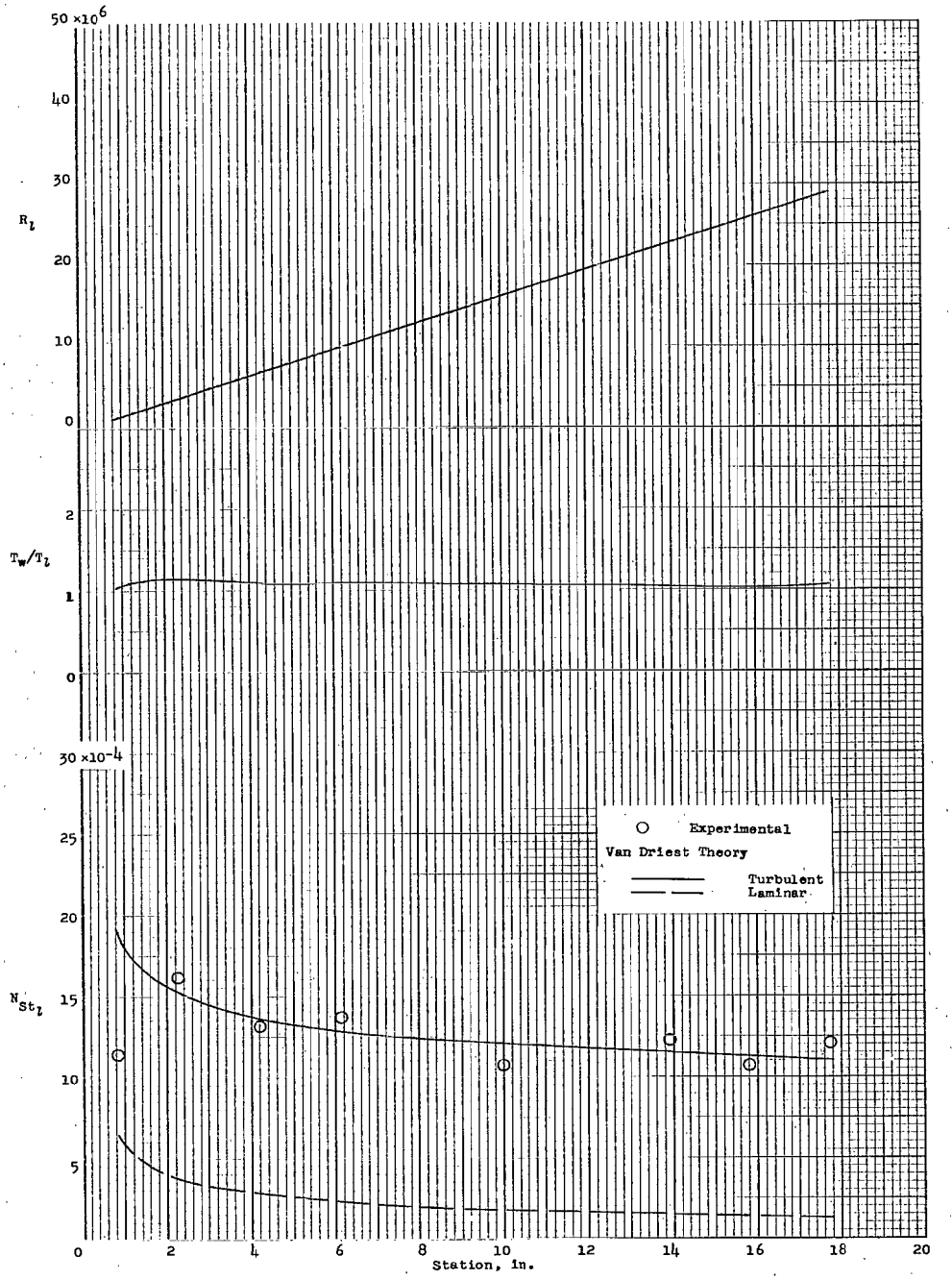

(c) t = 4.8 seconds; M_∞ = 2.25.

Figure 13.- Continued.

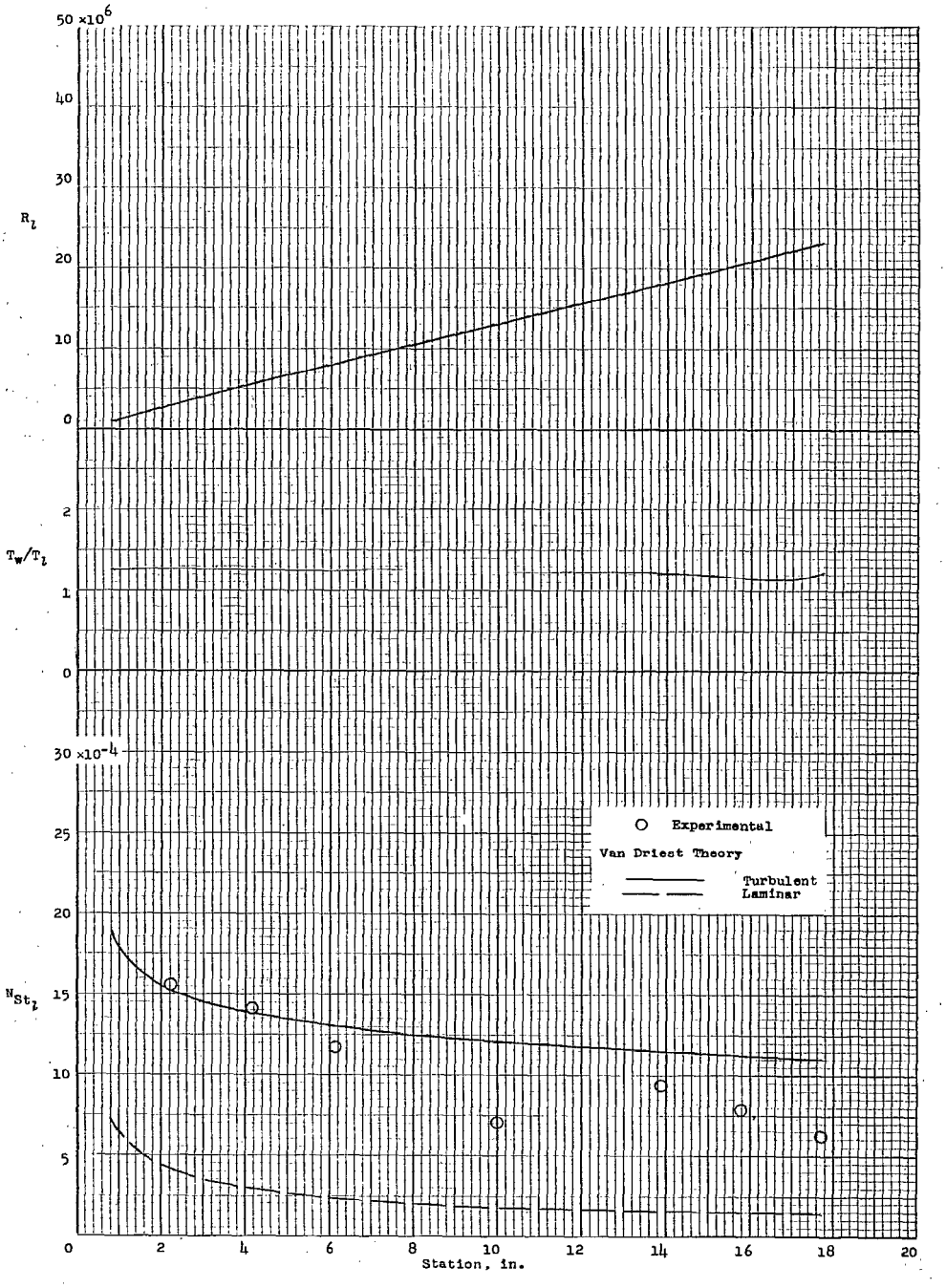

(d) $t = 7.8$ seconds; $M_\infty = 2.24$.

Figure 13.- Continued.

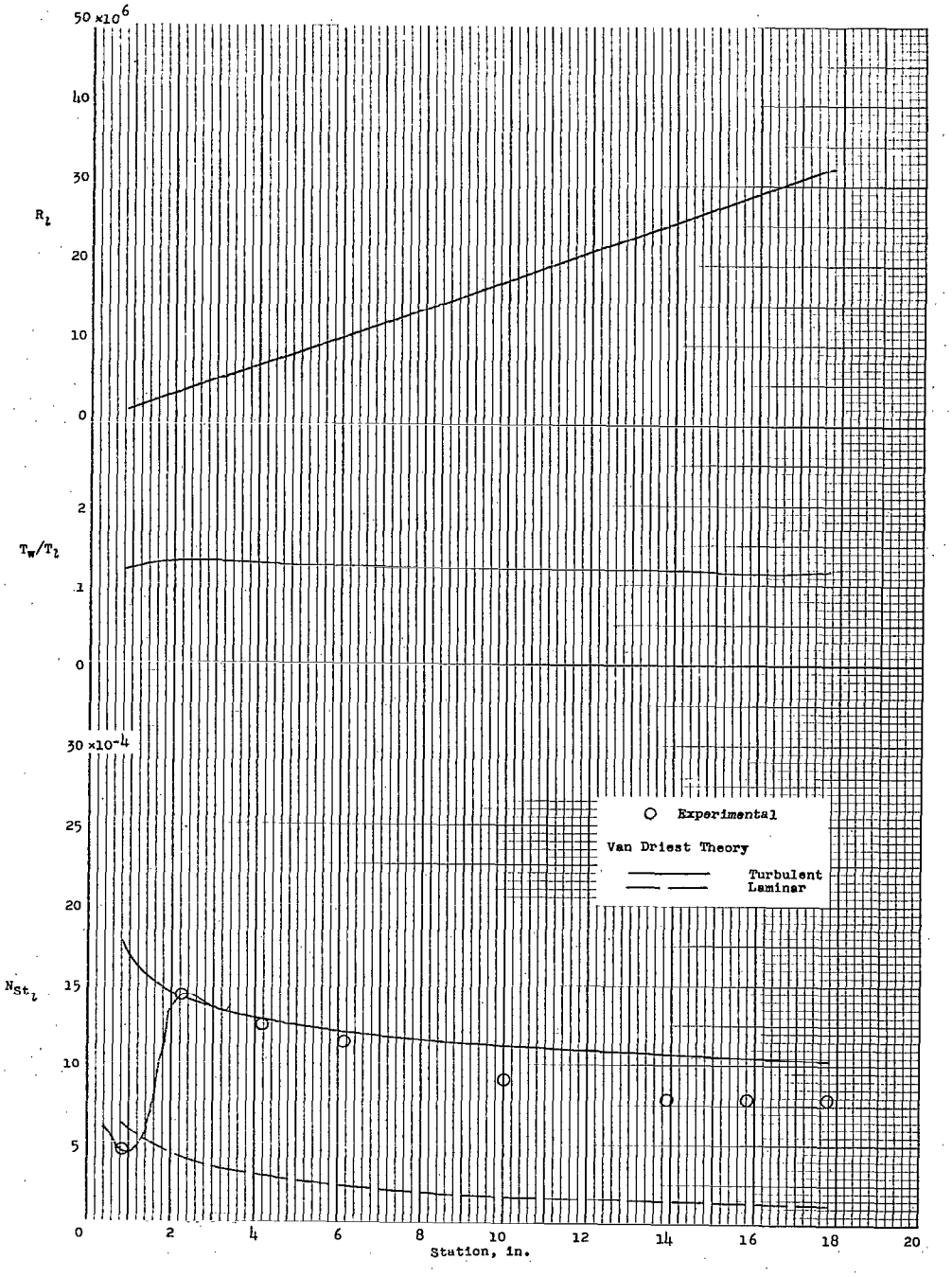

(e) t = 8.4 seconds; M_∞ = 2.87.

Figure 13.- Continued.

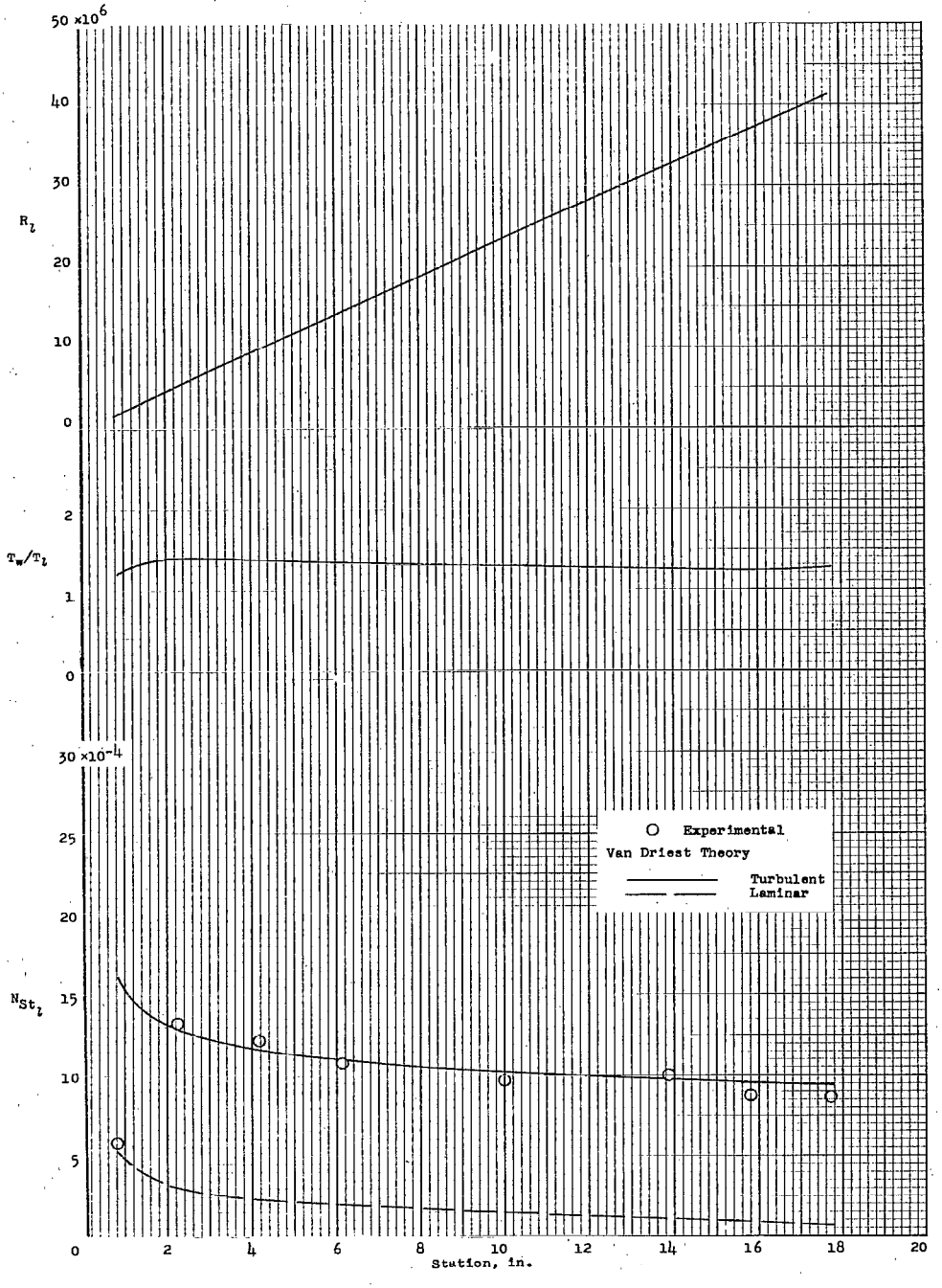

(f) t = 9.0 seconds; M_∞ = 3.50.

Figure 13.- Continued.

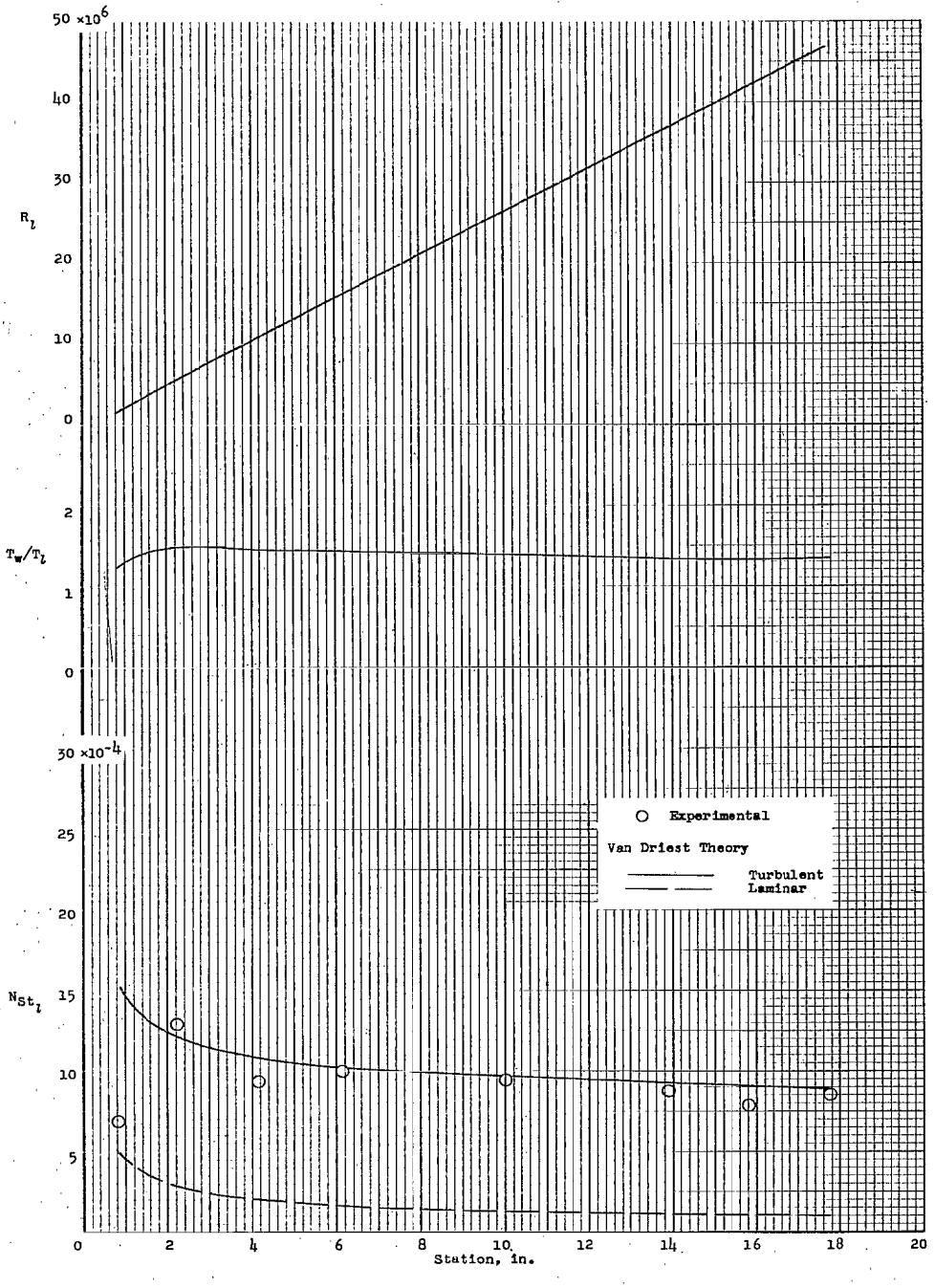

(g) t = 9.4 seconds; M_∞ = 3.97.

Figure 13.- Concluded.

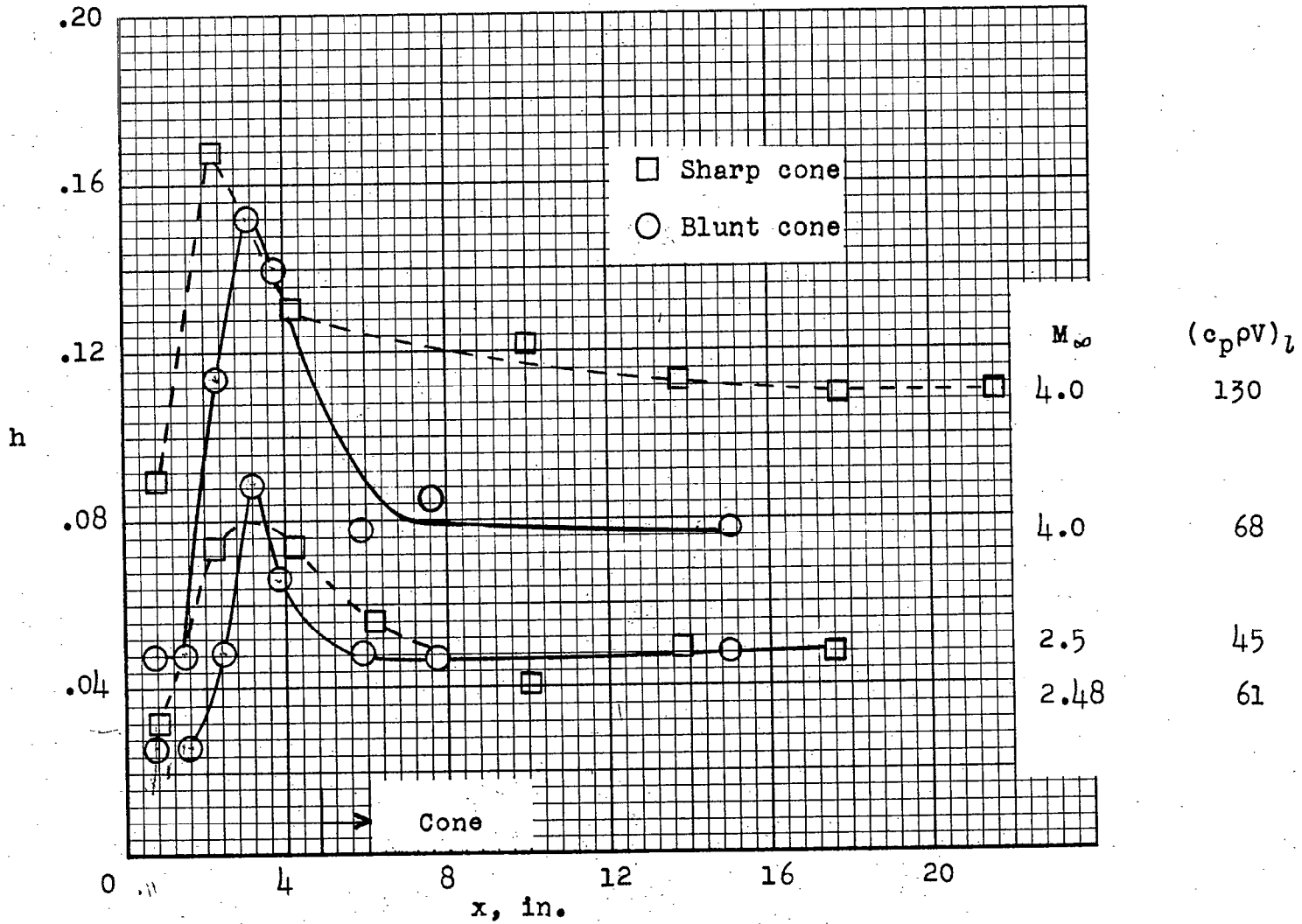

Figure 14.- Comparison of turbulent heat transfer for sharp and blunt cones.